Mine Water and the Environment (2020) 39:535–555
https://doi.org/10.1007/s10230-020-00655-0

TECHNICAL ARTICLE

Microbial Geochemistry of the Acidic Saline Pit Lake of Brunita Mine (La Unión, SE Spain)

Javier Sánchez-España[1] · Iñaki Yusta[2] · Andrey Ilin[2] · Charlotte van der Graaf[3] · Irene Sánchez-Andrea[3]

Received: 28 June 2019 / Accepted: 12 January 2020 / Published online: 25 January 2020

Abstract

We present the first study of a unique acidic lake formed in the Brunita open pit (La Unión mines, Cartagena, SE Spain). This pit lake exhibits chemical characteristics typical of AMD, such as low pH (pH 2.2–5.0) and high iron content (500–6400 mg/L total Fe). It also has some of the highest sulfate concentrations reported to date in pit lakes (26,000–38,400 mg/L SO_4^{2-}) and transition metals like Mn (up to 2000 mg/L), Zn (500 mg/L), or Cu (250 mg/L). In addition, we found abnormally high concentrations of salt-forming ions (e.g. 5500 mg/L Mg, 750–1300 mg/L Cl, and 300–630 mg/L Na). The resulting high salinity (58‰) at the bottom creates a meromictic lake despite the lake's low relative depth (9%), with an anoxic, reducing monimolimnion isolated from the oxygenated mixolimnion. In the monimolimnion, we observed decreased metal concentrations (e.g. Cu, Zn, Cd, Cr, Pb, Th). We hypothesize that these metals are being removed by interaction with biogenic H_2S and subsequent precipitation as metal sulfides. Scanning electron microscopy shows sub-micron, spherical particles of ZnS in close association with cocci and rod-like bacteria. Analysis of the microbial community composition through 16S rRNA gene amplicon sequencing revealed different genera of sulfate-reducing bacteria (SRB) in the monimolimnion, including *Desulfobacca*, *Desulfomonile*, *Desulfurispora*, and *Desulfosporosinus*. Their apparent ability to reduce sulfate and selectively precipitate potentially toxic metals, and their resistance to this lake's extreme geochemical conditions, makes these bacteria of great interest for biotechnological applications (e.g. bioremediation and biomining).

Keywords Acidic mine pit lakes · Metal pollution · Bacterial sulfate reduction · Natural attenuation

Introduction

Acidic pit lakes formed in metal mines are singular water bodies that exhibit, at the same time, (1) geochemical and biological features typical of acid mine drainage (i.e. low pH, high metal and sulfate concentrations, and low microbial diversity, mostly composed of acidophiles) and (2) physical, limnological, and hydrological processes common to both man-made reservoirs and natural lakes (e.g. alternation of seasonal stratification with turnover periods, vertical fluxes of solutes and sediments, eddy diffusion, sediment/water interaction, a food chain with eukaryotic primary producers in the photic zone and prokaryotic decomposers in the bottom part; Geller et al. 2013a, b). These artificial lakes are complex aqueous systems where research fields such as geochemistry, microbiology, microbial ecology, physical limnology, hydrology, mineralogy, and sedimentology need to be combined for a complete understanding (Geller et al. 2013a, b; Sánchez-España et al. 2008; Schultze et al. 2017). Scientific research conducted in these environments can help improve remediation/prevention practices used by mining companies and regulatory agencies.

Recent investigations in pit lakes have provided useful insight about biogeochemically relevant aspects, such as the photoreduction of dissolved and colloidal ferric iron at low pH (Diez-Ercilla et al. 2009), solubility of nanocrystalline

✉ Javier Sánchez-España
j.sanchez@igme.es

Iñaki Yusta
i.yusta@ehu.eus

Irene Sánchez-Andrea
irene.sanchezandrea@wur.nl

[1] Geochemistry and Sustainable Mining Unit, Dept of Geological Resources, Spanish Geological Survey (IGME), Calera 1, Tres Cantos, 28760 Madrid, Spain

[2] Dept of Mineralogy and Petrology, Basque Country University (UPV/EHU), Apdo. 644, 48080, Bilbao, Spain

[3] Laboratory of Microbiology, Wageningen University, Stippeneng 4, 6708 WE Wageningen, The Netherlands

oxyhydroxysulfates (Sánchez-España et al. 2011), cycling of Fe and S through the water column and sediments (Falagán et al. 2014; Wendt-Potthoff et al. 2012), sulfidogenesis in transitional chemoclines (Diez-Ercilla et al. 2014), development of staircase-like stratification (Sánchez-España et al. 2014a), dynamics and accumulation of carbon dioxide in deep layers (Sánchez-España et al. 2014b), or discovery of novel bacterial species with potential biotechnological interest (Falagán et al. 2016, 2017a; Falagán and Johnson 2014, 2015). The latter issue is of particular importance, since the extreme physicochemical conditions imposed on microorganisms in these aqueous environments means they can be considered poly-extremophiles, capable of simultaneously coping with different environmental stressors. These include: (i) extreme acidity (very low pH), (ii) extreme salinity (very high ionic strength), (iii) very high concentrations of different highly toxic metals, and (iv) oligotrophy (low nutrient availability). This simultaneous resistance to multiple extreme conditions makes poly-extremophiles of great biotechnological interest in e.g. bioremediation or biomining.

The main purpose of this study was to test the likelihood of our hypothesis that SRB mediate the physicochemical changes observed at the bottom layer of the Brunita pit lake. For that, we first performed an in-depth physicochemical characterization of the water column, and then investigated the microbial community composition in its different layers.

Site Description and Environmental Framework

The Brunita open pit mine (37°36′1 N, 0°53′23″ W, 132 m above sea level) is situated 2 km to the south of the mining town of La Unión, and 6 km to the east of the city of Cartagena, in the province of Murcia (SE Spain) (Fig. 1). Brunita mine was one of the most important mines in the *La Unión-Sierra de Cartagena* mining district (García 2004; Oen et al. 1975). The Sierra de Cartagena Mountain Range is a low altitude, small coastal area with semiarid Mediterranean climate, characterized by the tectonic superposition of thrust sheets related to the convergence between African and Iberian plates during Tertiary times. The mineralization was a stratiform orebody dominated by pyrite (FeS_2), sphalerite (ZnS) and galena (PbS), with other minor sulfides like marcasite (FeS_2), pyrrothite (FeS) and arsenopyrite (FeAsS) (Pavillon 1969; Robles-Arenas et al. 2006). The mine was mainly exploited for the extraction of Zn and Pb (Manteca and Ovejero 1992), though pyrite was also eventually mined at minor scale for the production of sulfuric acid (Cánovas et al. 2013). Sulfide minerals are associated to a paragenesis composed of quartz, chlorite and carbonate-containing minerals like siderite, dolomite and minor calcite (Oen et al. 1975; Robles-Arenas et al. 2006). The orebody was firstly exploited as an underground mine by the mining company Minera Celdrán at the beginning of the twentieth century, but in the mid-1980s, the French company Peñarroya bought the mine and transformed it into an open pit mine which started ore extraction in 1985 (Cánovas et al. 2013). Mining operations conducted on site included run-of-mine reduction, waste dumping in mining voids and open pits and a flotation plant in the Portman Bay which used seawater for metallurgical processing (García 2004; López-García et al. 2010). However, this pit was exploited during a very short time period, closing definitively in 1988. Decreasing prices in the metal market and the high maintenance costs derived from the need of continuous pumping to avoid mine flooding were apparently major reasons determining mine closure.

This abandoned mining site is now best known for its deep red, acidic pit lake resulting from the pit flooding. This lake presently has a surface area of 45,000 m^2, a maximum depth of 22 m, and a relative depth (defined as the ratio of the maximum depth as a percentage of the mean diameter of the lake at the surface, according to Wetzel 2001) of 9%. This mining landscape is also famous among mineral collectors for the occurrence of high quality specimens of minerals like vivianite [$Fe_3(PO_4)_2{\cdot}8H_2O$] and some rare mineral species like ludlamite [$(Fe, Mg, Mn)_3(PO_4)_2{\cdot}4H_2O$] or cronstedtite [$Fe_3^{2+}Fe^{3+}(Si, Fe)_2O_5(OH)_4$] (Cánovas et al. 2013; López-García et al. 1992). Numerous residues and piles of mine waste and tailings still exist in the surroundings of the mine pit, along with the ruins of former mining buildings (Fig. 1). Gypsum ($CaSO_4{\cdot}2H_2O$) is conspicuous in the pit lake and can be observed in close contact with the water (Fig. 2a), and also below the water table (Fig. 2b), suggesting direct precipitation by solubility saturation. Efflorescent sulfate salts are also common in evaporative pools adjacent to the lake (Fig. 2c). However, the pit lake is not totally devoid of biological activity, and eukaryotic photosynthetic microorganisms are usually observed in the lake shore in close contact with oxygen bubbles (Fig. 2d).

Materials and Methods

Field Work and Sample Collection

Four field campaigns took place in December 2017, May 2018, November 2018, and July 2019. Physico-chemical profiling was conducted with a Hydrolab MS5 multi-parametric probe (Hach®, Loveland, CO, USA) properly calibrated following manufacturer's instructions. Field parameters measured in the aqueous phase included pH, oxidation–reduction potential (ORP), temperature (T), dissolved oxygen concentration (DO), specific conductivity (SpC), and total pressure of dissolved gases (TDG). In addition to these parameters,

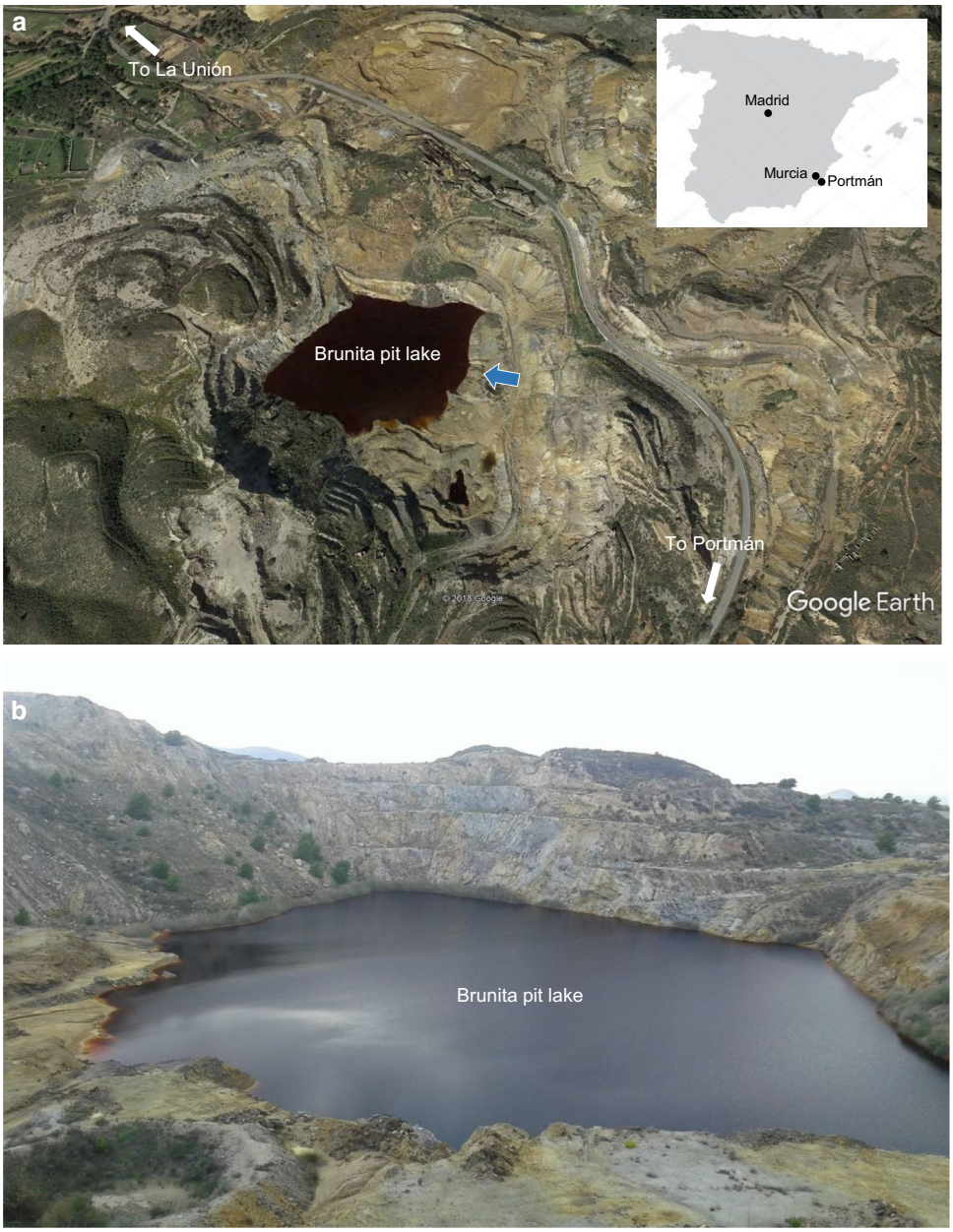

Fig. 1 Views of Brunita acidic pit lake (La Unión mines, Cartagena, SE Spain): **a** Satellite view (Google Earth image), and **b** panoramic view (field photograph taken from point marked by arrow in picture a)

water turbidity (in nephelometric turbidity units, NTUs) was also measured in July 2019 with a HI 93414 portable turbidity meter (previously calibrated on site) from Hanna Instruments, S.L. (Eibar, Spain).

In three of these four campaigns (Dec 2017, May 2018, and Nov 2018), water samples from different depths (0, 2, 12, 15, and 17 m) were collected for chemical analyses with a 5 L Van Dorn® sampling bottle (KC Denmark) (Fig. 2e, f). Volumes of 125 mL were filtered on site with 0.45 µm nitrocellulose membrane filters (Merck Millipore®, Burlington, Massachusetts, USA), stored in 125 mL polyethylene bottles, acidified with 0.4 mL of HCl 1 M, and cool-preserved during transport. Filters coated with suspended particulate matter (SPM) were also obtained from the same depths by filtering 250 mL of additional water. These filters were immediately washed by further filtration of 50–100 mL of ultra-pure deionized water (MilliQ), kept in closed Eppendorf vials (4 mL), and stored at 4 °C until their chemical and mineralogical characterization in the laboratory.

To investigate the microbial community composition, water from 2, 12, and 17 m was filtered through 0.2 µm pore size-Sterivex filters (Merck Millipore®) encapsulated with a Luer-Lock® flow system during the December 2017 sampling campaign. These filters were used in the lake shore using sterile materials (e.g. syringes, tubing, vials) and RNase AWAY reagent solution (ThermoFisher Scientific) to decontaminate apparatus, glassware, and plastic ware. To ensure a sufficient biomass for DNA extraction, a variable

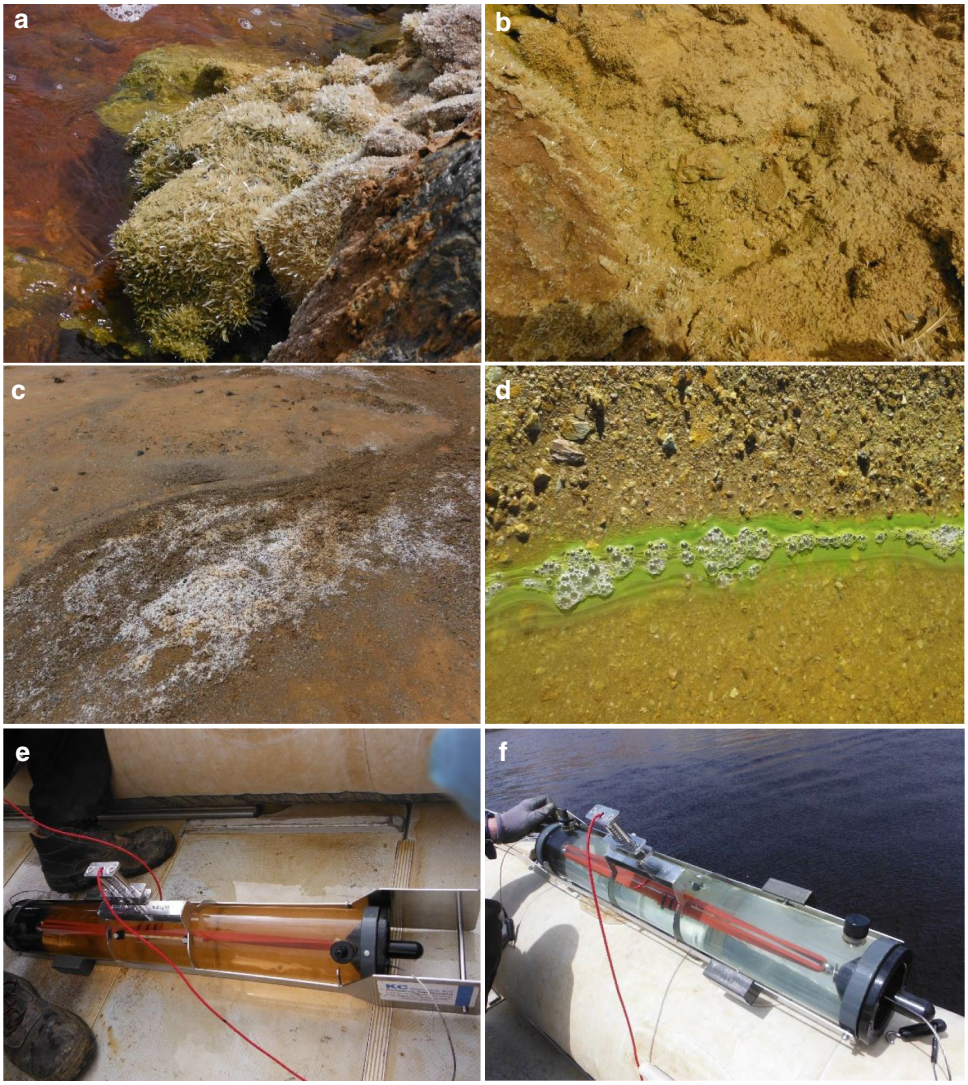

Fig. 2 Field pictures showing remarkable features of the Brunita acidic pit lake: **a** Formation of abundant gypsum crystals on rock surfaces or **b** directly below the water surface; **c** presence of efflorescent sulfate salts near the lake shore; **d** photosynthetic green algae in the shore of the lake (pH 2.1), with abundant oxygen bubbles; detail of the Van Dorn limnologic bottle after collecting water from the Fe(III)-rich mixolimnion (note dark red color and turbidity) (**e**) and water from the Fe(II)-rich monimolimnion (note the colorless, transparent water) (**f**)

volume (between 2 and 3 L, depending on water depth) was filtered until saturation (clogging) was reached. These filters were sealed and preserved at − 20 °C on dry ice until arrival at the Laboratory of Microbiology in the University of Wageningen.

A sediment sample was taken from the pit lake bottom in the area of maximum depth (22 m) with a dredger, then transferred to a sealed plastic box and transported to the lab for further chemical and mineralogical analyses.

Chemical Analyses of Water and Sediment

Ion concentrations of the water samples were analyzed by atomic absorption spectrometry (AAS) (Na, K, Ca, Mg), inductively coupled plasma-atomic emission spectrometry (ICP-AES) (Al, Fe, Mn, Cu, Zn, SO_4^{2-}, and SiO_2), and inductively coupled plasma-mass spectrometry (ICP-MS) (As, Cr, Pb, Co, Ni, Cd, Se, U, Th) using Varian SpectrAA 220 FS, Agilent 7500ce, and Varian Vista MPX instruments, respectively. The analytical detection limits were < 1 mg/L for major metals and < 1 µg/L for trace elements. Nitrate and ammonium nitrogen, as well as phosphate phosphorus, were analysed with a UV–VIS DR2800 spectrophotometer (Hach, Loveland, CO, USA) using cuvette tests LCK 339, 304, and 348, respectively (see Wendt-Potthoff et al. 2012). Total organic carbon (TOC) was analysed in a Shimadzu TOC-VCPH elemental analyzer.

Mineralogical identification of one sediment sample was performed by X-ray diffraction (XRD) on a PANalytical X'Pert Pro diffractometer. XRD conditions included Cu K_α radiation (40 kV, 40 mA), graphite monochromator, and a PIXcel detector. This sample was also chemically analyzed by X-ray fluorescence (XRF) for major oxides (given in wt%) and by ICP-MS and AAS (after previous acid digestion) for trace elements (given in ppm or mg/kg dry weight). Scanning electron microscopy (SEM) and transmission electron microscopy (TEM) on SPM were conducted at the SGIker facilities (UPV/EHU) using a JEOL JSM-7000F field

emission scanning electron microscope working at 20 kV. Images and compositional analyses by energy dispersive spectroscopy (EDS) were carried out on samples adhered to carbon-tape, placed in graphite mounts, and carbon-coated. TEM images and selected area electron diffraction (SAED) analyses of sulfide particles were performed on a Philips CM200 microscope after placing 2–3 drops of an ethanol suspension with the fine precipitates on lacy carbon films.

Microbial Community Analysis

Sterivex filters were transferred to bead tubes and DNA was extracted using the FastDNA Spin Kit for Soil (MP BIOmedicals, OH, USA) according to manufacturer's instructions. DNA concentration was measured using a Qubit 2.0 fluorometer (Thermo Fisher Scientific, Darmstadt, Germany), using the Qubit dsDNA BR assay kit (Invitrogen, Thermo Fisher Scientific, Darmstadt, Germany). The PCR reaction volume was 50 µL, consisting of 10 µL 5X HF buffer, 200 µM of each dNTP, 10 µM barcoded forward 515F (5′-GTGYCAGCMGCCGCGGTAA-3′) and reverse 806R (5′-GGACTACNVGGGTWTCTAAT-3′) primers, 2 U/µL Fusion Hot Start II DNA polymerase, and 0.4 ng/µL DNA template. An annealing temperature of 56 °C and 25 amplification cycles were used. PCR was performed in triplicate, and triplicate reactions were pooled for further processing. Negative controls were included with water instead of DNA as a template. Clean-up of pooled PCR products was performed using magnetic beads with CleanNA PCR kit (GC Biotech BV, The Netherlands) and DNA concentrations of cleaned product were determined on a Qubit 2.0 fluorometer (Thermo Fisher Scientific, Life Technologies, Darmstadt, Germany). Amplicons were sequenced with HiSeq 150 bp paired-end read sequencing (GATC Biotech, Konstanz, Germany).

Sequencing reads were processed on the Galaxy platform using the NG-Tax pipeline (Ramiro-Garcia et al. 2018). Amplicon 16S rRNA gene sequences were clustered into operational taxonomic units (OTUs) with > 98.5% sequence similarity. Taxonomy was assigned using the SILVA SSU rRNA database (v132) (Quast et al. 2013; Yilmaz et al. 2014). OTU abundance was expressed as a fraction of total reads after removal of eukaryotic sequences classified as chloroplasts or mitochondria. A cut-off of 2% of total reads was applied for the OTU's representation in results, except for taxa previously identified as important in iron and sulfur cycling in AMD environments.

Water/mineral Equilibrium Calculations

We used PHREEQC (version 3.0.5-7748; Parkhurst and Appelo 2013) to calculate saturation indexes (SI) of common sulfide minerals, as well as aluminum oxy-hydroxides and some other mineral phases with potential solubility control on certain metals at the conditions in the Brunita pit lake. We considered the physico-chemical parameters measured on site (e.g. pH, ORP, T, DO) and all ionic species measured in the pit lake waters. The ionic strength of the water was between 0.60 and 0.76, which is close to that of seawater, which is usually considered the limit for application of the Davies equation of ionic activity coefficients in dilute solutions (Nordstrom 2004; Sánchez-España and Diez 2008). All calculations were made using the Wateq 4 f.dat thermodynamic database (Ball and Nordstrom 1991).

Results and Discussion

Physico-chemical Characteristics

The profiles shown in Fig. 3 show a sharply stratified pit lake. A 2 m thick chemocline situated between 12 and 14 m depths separates an upper, oxygenated layer from a lower anoxic and reducing layer with pronounced vertical gradients of dissolved substances, as indicated by specific conductivity (Fig. 3b). The oxycline separating both layers is thinner (≈ 1 m thick) and displaced around 1 m upwards with respect to the chemocline (11–12 m depth interval) (Fig. 3e). The redoxcline is coincident with the chemocline at 12–14 m depth (Fig. 3d). Although the observation window is still limited and winter depth profiles are lacking, some geochemical features like the sharp conductivity and pH gradients, the important increase of dissolved gases (as deduced from the TDG profile, Fig. 3f), and the extremely high concentrations of reduced substances like ferrous iron (Fig. 4b), make us assume that this pit lake is meromictic and, thus, stratified year round (so the terms mixolimnion and monimolimnion are used hereafter to refer to the upper and lower layer, respectively).

The mixolimnion tends to be thermally homogeneous and almost fully mixed in the late fall or early winter (with just some subtle vertical variations of temperature or DO; Fig. 3a) and experiences strong thermal stratification during late spring and summer, when a warmer epilimnion (usually comprising the upper 2 m of the water column) forms as a result of enhanced solar heating and related evaporation (Fig. 3a). The thermal anomaly observed in July 2019 (water temperatures around 30 °C at 2 m below colder water; Fig. 3a) was caused by a long period of warming during the summer followed by a sudden and extraordinarily intense period of heavy rains, which provoked the formation of an upper and less saline layer due to the entrance of meteoric water (Fig. 3b). The pH highly differs between the epilimnion, which is very acidic (between pH 2.0 and 2.6, with some seasonal variability), and the monimolimnion,

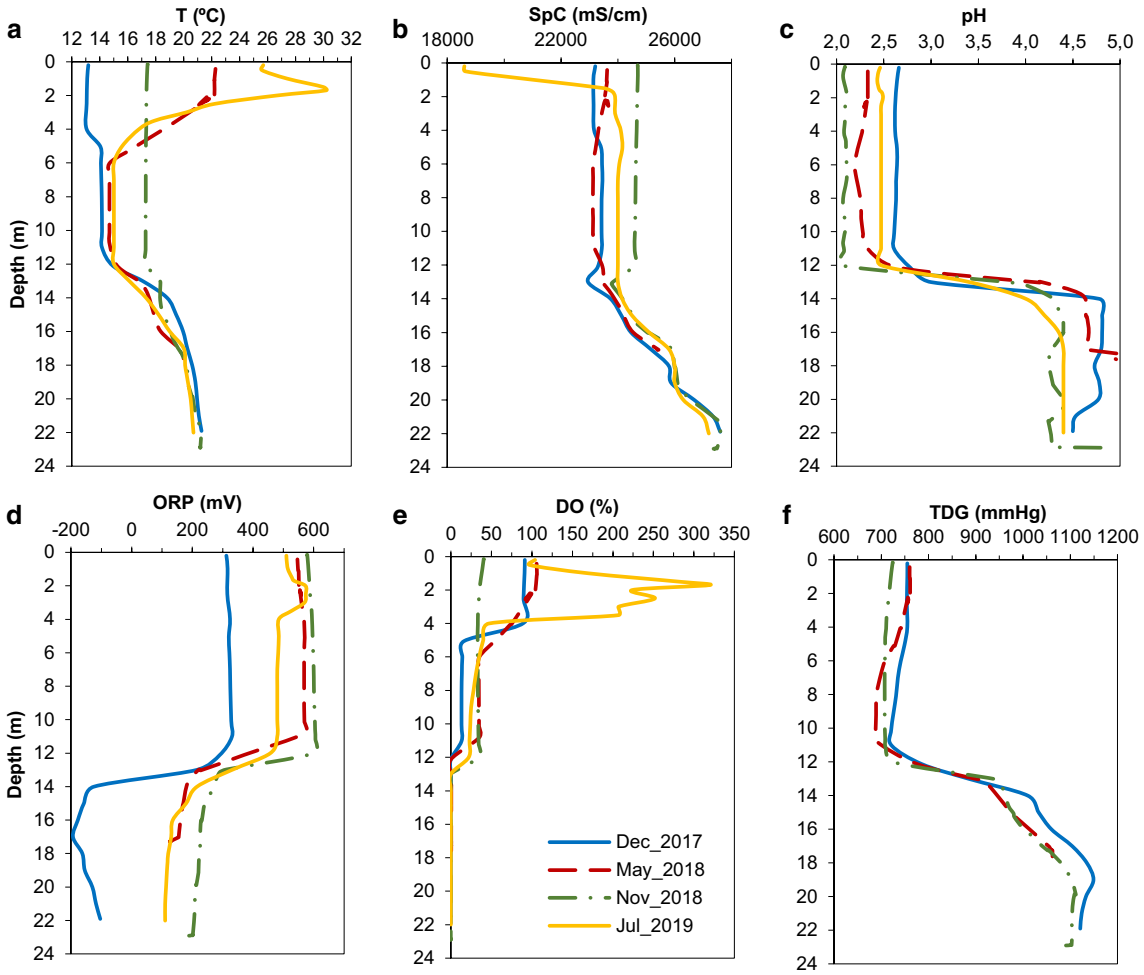

Fig. 3 Depth profiles of physico-chemical parameters in Brunita acidic mine pit lake [temperature (T), specific conductance (SpC), pH, oxidation–reduction potential (ORP), dissolved oxygen saturation (DO), and total dissolved gas pressure (TDG)]

where the pH remarkably increased to between 4.5 and 5.0 (Fig. 3c).

Oxygen concentrations show sharp seasonal variations in the mixolimnion during the year (Fig. 3e). The DO was near saturation in the epilimnetic waters in December 2017 and May 2018, but was present at rather low concentrations around 2.5–3.0 mg/L of O_2 (equivalent to 30–40% sat.) in November 2018, and was virtually absent in the deep part in December 2017. These low DO concentrations in the mixolimnion reflect important oxygen consumption in the winter, likely due to decomposition of the organic matter produced during the summer months by primary production, as described below. In contrast, a marked peak of DO saturation (reaching peak values of 320% sat., which is equivalent to 22 mg/L O_2 at the corresponding temperature) was observed at around 2 m in July 2019 (Fig. 3e). This peak coincided with the concentration of phytoplanktonic algae in this layer, which was visible to the naked eye, suggesting the development of an algal bloom and an accompanying increase of photosynthetic activity in this period. In the monimolimnion, DO was totally absent, and ORP values were always below 300 mV and as low as −200 mV at 17 m depth (e.g. December 2017; Fig. 3d).

The TDG profile also reveals a sharp gradient in the total pressure of dissolved gases, which is another consequence of the perennial isolation of the bottommost water layer from the rest of the water column (Fig. 3f). This parameter is constant in the mixolimnion at values of ≈725–750 mm Hg (1 bar), which denotes equilibrium with the atmosphere. Once below the redoxcline/chemocline, TDG increases towards the lake bottom to values up to 1100–1150 mm Hg (1.5 bar) which suggests a significant increase of dissolved gases. Given that the layer is totally devoid of oxygen (Fig. 3e), this increase of dissolved gas is likely due to the input of carbon dioxide (CO_2 aq.), which can be produced by either biological activity (i.e. anaerobic bacterial metabolism) or abiotically through water/rock interaction (e.g. acid dissolution of carbonate minerals), as discussed below.

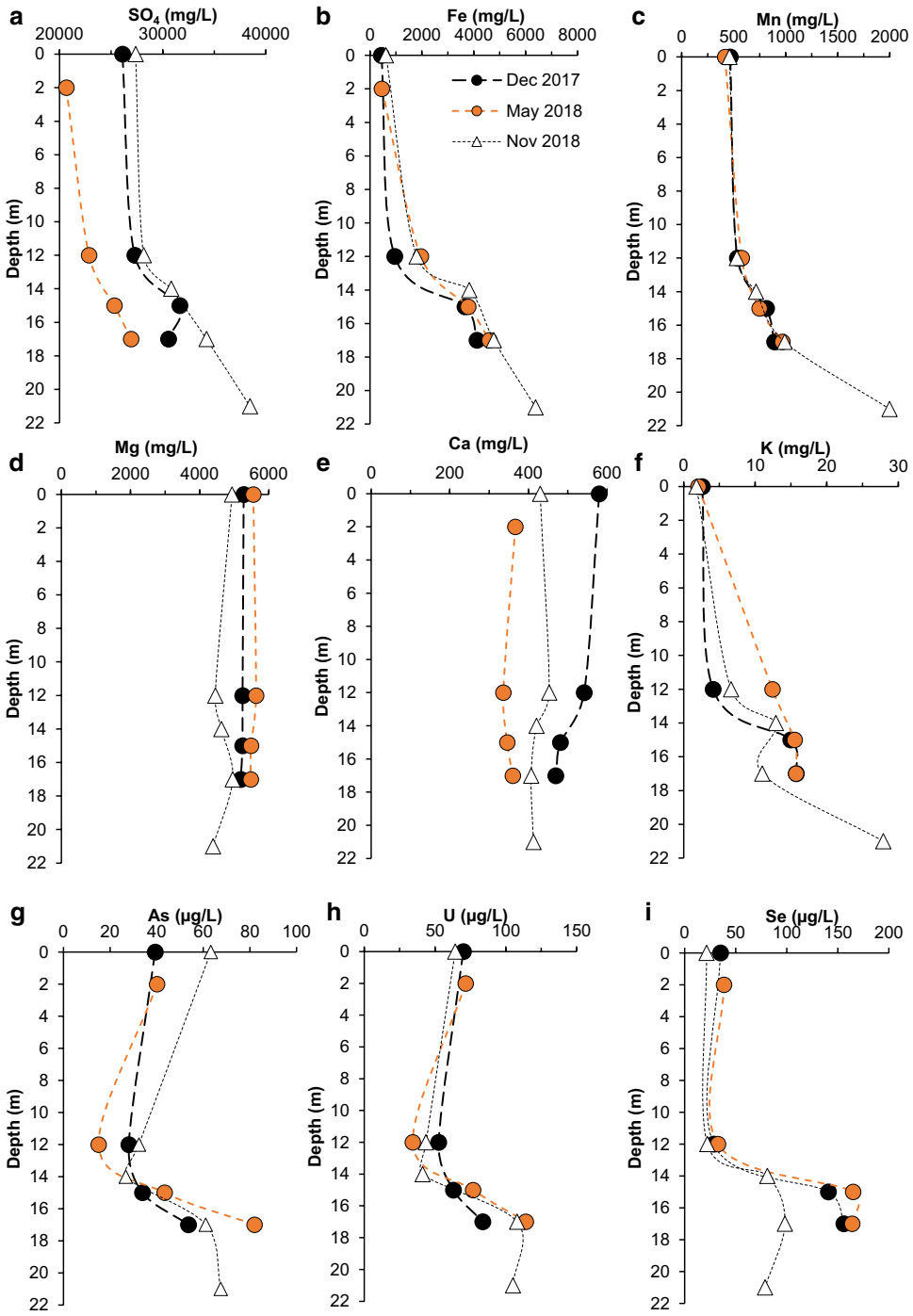

Fig. 4 Depth profiles of element concentration for some major ions (SO_4^{2-}, Fe, Mn, Mg, Ca, K) and selected trace elements (As, U, Se) showing apparent conservative behavior in the acidic pit lake of Brunita mine

Water Chemistry

The major ion and trace metal concentrations allow classification of the dissolved substances into two groups depending on their geochemical behavior. The elements that we refer to as *conservative* have nearly constant concentrations at all depths (e.g. Mg, Ca; Fig. 4) or notably increase with depth (e.g. SO_4, Fe, Mn; Fig. 4). Thus, they are apparently not affected by the major geochemical or biological processes that cause the removal of other, more *reactive* elements from the aqueous phase. In some cases (e.g. Mg), the element is not involved in any major reaction, whereas in other cases, the element may be involved in some process (e.g. Ca and SO_4 in gypsum precipitation), but because the element is present in excess, its aqueous concentration is not significantly affected. Alternatively, the elements increase in concentration with depth as a natural consequence of mineral dissolution (e.g. SO_4 or Fe, due to pyrite dissolution), which

is much more important at depth, given the funnel-shaped geometry of most open pits and the associated lower water-to-rock ratio (Sánchez-España et al. 2008, 2009).

Many other elements decrease in concentration with depth (Figs. 5, 6). These elements are participating in different geochemical and microbially mediated processes (discussed below) and are therefore considered *reactive* elements. This is the case for some major substances like SiO_2, Al, or Cu (Fig. 5), and many trace metals (e.g. Cd, Cr, Pb, Th, Ni, Co; Fig. 6). The case of Zn is noteworthy since this element shows a concentration increase immediately below the chemocline, but then shows a slight decrease near the lake bottom (Fig. 5). Sodium and chloride are also included in this category for simplification, although these elements are actually not reactive and their vertical variations is due to reasons other than chemical or biological reactivity, as explained below.

Conservative Elements

Sulfate and iron are the most abundant of the conservative elements due to the oxidative dissolution of pyrite, which is the most abundant sulfide in the open pit (Cánovas et al. 2013). The peak values found at the lake bottom (38,400 mg/L SO_4^{2-} and 6400 mg/L Fe) are among the highest recorded in any pit lake of the world (Table 1; Eary and Castendyk 2013; Sánchez-España et al. 2008). When expressed in molar units, these concentrations indicate

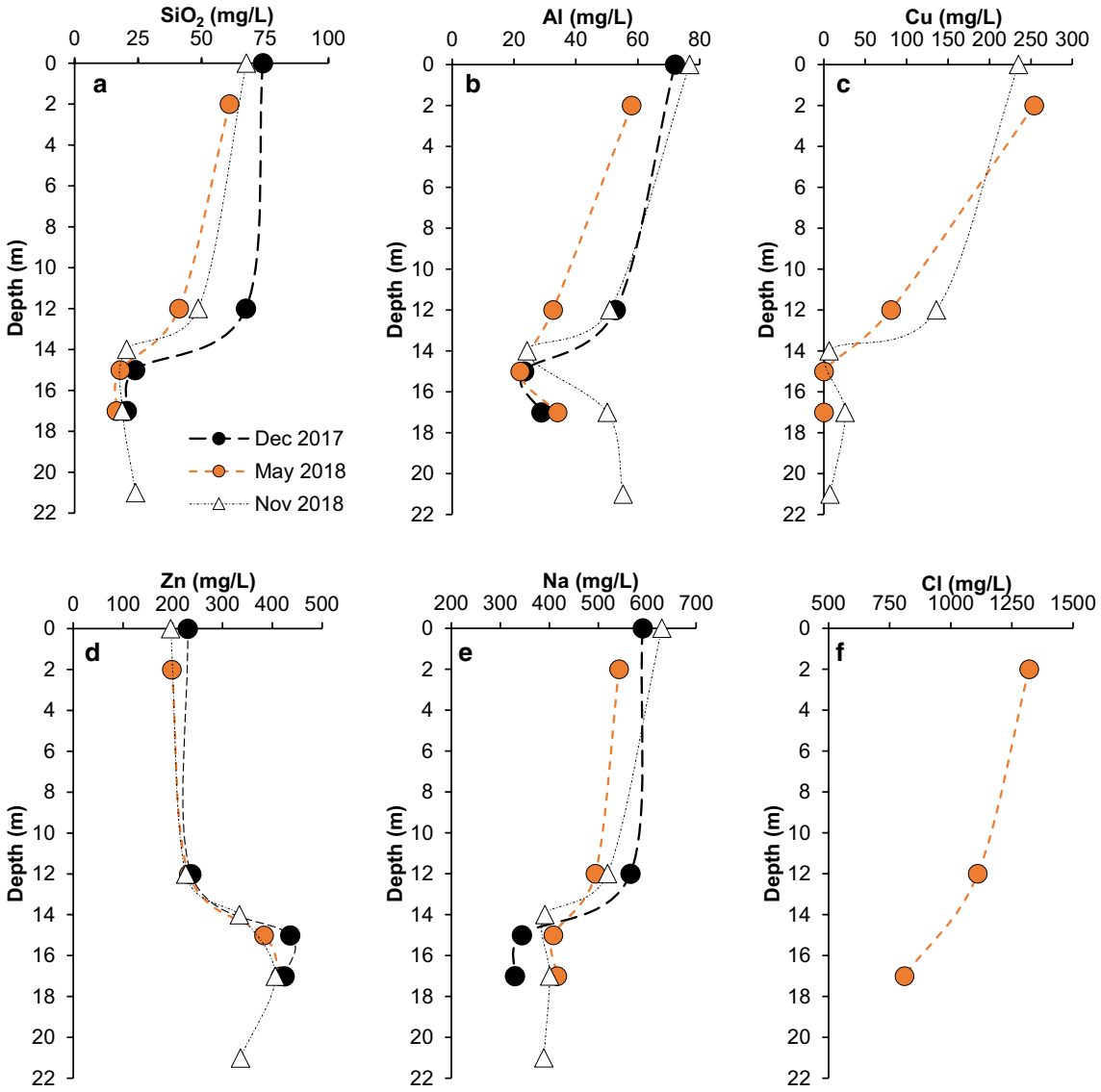

Fig. 5 Depth profiles of element concentration for some major dissolved substances (including SiO_2, Al, Cu, Zn, Na, and Cl) showing apparent reactive behavior in the acidic pit lake of Brunita mine

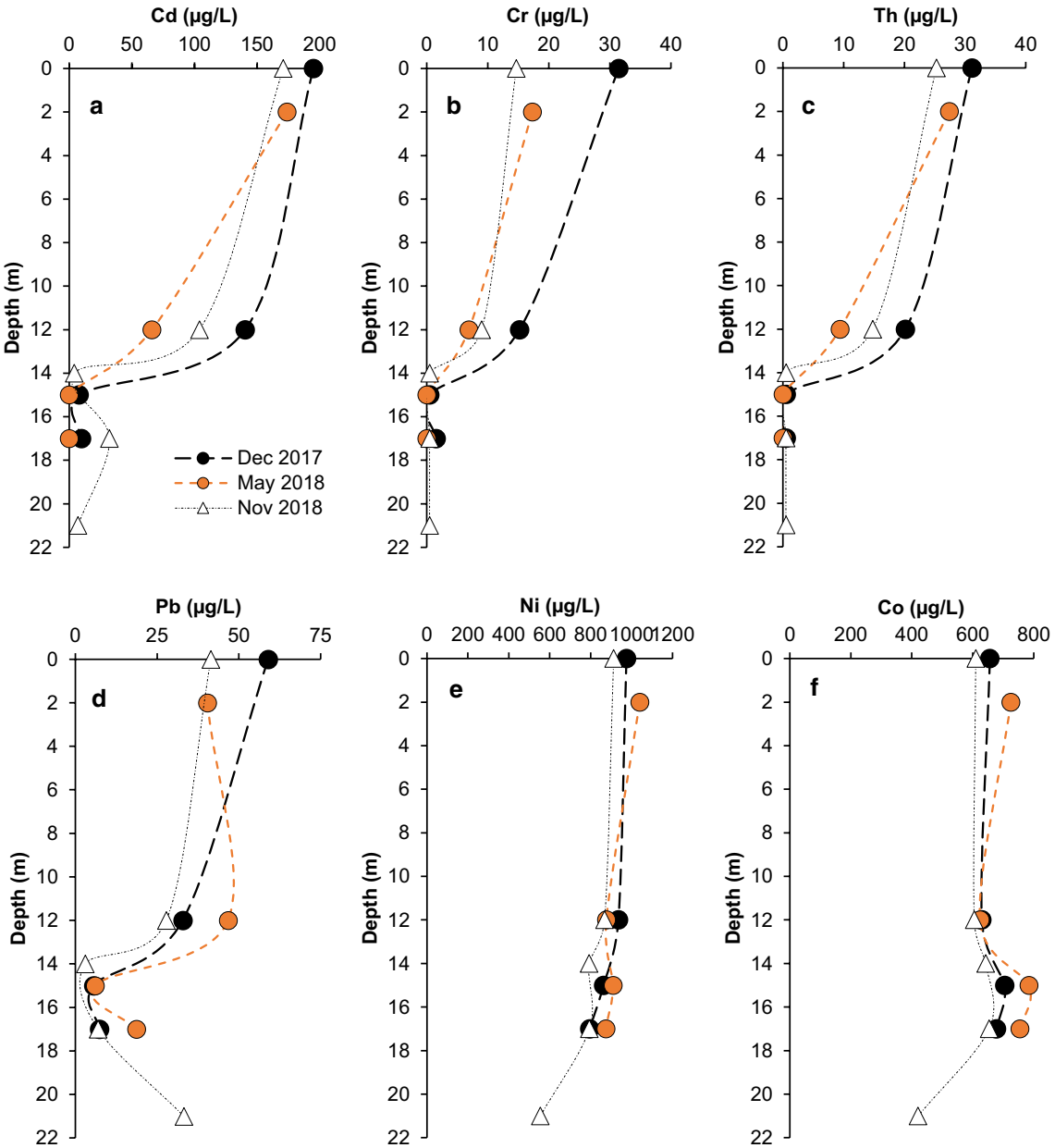

Fig. 6 Depth profiles of element concentration for selected trace metals (Cd, Cr, Th, Pb, Ni, Co) showing apparent reactive behavior in the acidic pit lake of Brunita mine

a [Fe/S] molar ratio of 0.12–0.33 in the upper part and 0.65–0.87 at depth (*not shown*). In both cases, this [Fe/S] ratio deviates from the value theoretically resulting from pyrite dissolution ([Fe/S] = 0.5). In the case of the oxygen-rich mixolimnion, the low [Fe/S] ratio may reveal the continuous removal of dissolved iron through Fe(III) precipitation. However, some excess of dissolved sulfate by the influence of seawater (e.g. via aerosols) or diffusion of saline waters from nearby tailings should not be ruled out. In the case of the anoxic monimolimnion, the higher [Fe/S] ratio could be suggesting an excess of dissolved iron due to dissolution of other Fe-bearing minerals, such as siderite ($Fe^{II}CO_3$), dolomite ($CaMg[CO_3]_2$), vivianite, ludlamite, or cronstedtite (Cánovas et al. 2013). Alternatively, this high [Fe/S] ratio could derive from sulfate removal via bacterial sulfate reduction to labile H_2S and later precipitation of metal sulfides (see below).

The concentration of dissolved manganese (2000 mg/L) in the bottom of the pit lake is the highest reported in a pit lake so far (Table 1; Eary and Castendyk 2013; López-Pamo et al. 2009; Sánchez-España et al. 2008), and is probably due to the dissolution of highly soluble Mn-bearing minerals,

Table 1 Comparison of concentrations of selected chemical constituents (in mg/L) between Brunita acidic pit lake and mine effluents of the IPB and pit lakes worldwide

	Brunita	IPB pit lakes[1]	IPB effluents[2]	WCLMPL[3]	AMMPL[4]	Berkeley[5]	Dombrovska[6]
Major ions							
SO_4^{2-}	26,000–38,500	2000–18,000	1000–20,000	0–8000	31–25,000	8000–9000	5000–80,000
Cl^-	750–1300	–	100–500	0–1300	–	< 50	20,000–160,000
Mg^{2+}	5500	33–1250	0–1000	0–300	0–2463	515	1000–30,000
Na^+	300–630	10–95	3–124	0–900	–	74	
Metals							
Mn^{2+}	500–2000	3–254	3–50	0–90	0–150	260	–
Zn^{2+}	200–440	6–550	0–300	0–90	0–46	638	–
Cu^{2+}	250	2–150	1–70	0–20	0–36	76–153	–

References: [1]Sánchez-España et al. 2008; [2] Sánchez-España et al. 2005; [3]Worldwide Coal and Lignite Mine Pit Lakes (Friese et al. 2013); [4]Australian Metal Mine Pit lakes (Kumar et al. 2013); [5]Gammons and Tucci 2013; [6]Zurek et al. 2018

such as Mn-siderite and ludlamite, which were present in the mine pit (Cánovas et al. 2013; Oen et al. 1975; Robles-Arenas et al. 2006).

The calcium concentration fluctuates between 350 mg/L (May 2018) and 600 mg/L Ca (December 2017), while the dissolved magnesium concentration is one of the highest reported for metal mine pit lakes, surpassed only by salt mines and alkaline pit lakes, such as Dombrovska in Ukraine (Table 1; Zurek et al. 2018). The abundance of Mg could be due to dissolution of Mg-rich phases like dolomite, siderite, or ludlamite. However, the molar ratio between calcium and magnesium ([Ca/Mg] = 0.05) is much lower than what would be expected from dolomite dissolution, which may imply partial removal of calcium from the aqueous phase by gypsum precipitation (Fig. 2a, b) and sources of magnesium other than carbonate (e.g. dolomite). As in the case of sulfate, some additional input of Mg from seawater-containing wastes dumped near the pit, can also be considered. Some other cations like potassium, and trace elements with potential toxicity, such As, U or Se, also show moderate increments in concentration at depth (Fig. 4g–i).

Reactive Elements

The reactive elements exhibit sharp concentration decreases below the redoxcline (Fig. 5). The case of Cu is the most intense, as it occurs at very high concentrations (240–250 mg/L) near the surface, and then it disappears from solution at depths below 14 m. Other elements are also notably diminished at depth, like silica (75 mg/L near surface to 25 mg/L SiO_2 below the redoxcline), sodium (600 mg/L Na to less than 400 mg/L), and chloride (1300 to 750 mg/L Cl). The aluminum profile shows a minimum at 14 m depth and then increases again towards the lake bottom (Fig. 5b).

These declines in concentration of some major elements are roughly coincident with a relative minimum observed in conductivity at around 13 m (Fig. 3b), and reveal partial loss of dissolved solids, possibly due to precipitation of insoluble mineral phases, as discussed below. The case of zinc is apparently contradictory because it suggests conservative behavior at first sight (Fig. 5). However, the slight decline shown at depth in the profile of November 2018 (from 440 mg/L Zn at 14 m to 340 mg/L at 21 m; Fig. 5), and the SEM observations on SPM (discussed below in a later section) indicate that this element is actually reactive and precipitating in the water column.

Among the trace metals showing apparent reactive behavior, some of them (e.g. Cd, Cr, Th) almost totally disappear from the aqueous phase in the deep layer (Fig. 6), whereas others exhibit a marked concentration minimum at 14 m and then increase again near the lake bottom (e.g. Pb), or show only a slight progressive decrease (e.g. Ni, Co).

Nutrient Content

Inorganic nitrogen is present as either nitrate or ammonium, while phosphorus is chiefly present as orthophosphate. The concentrations of both inorganic nitrogen and phosphorus are surprisingly high for an acidic pit lake, since these highly acidic water bodies tend to be oligotrophic (Wendt-Potthoff 2013). Inorganic nitrogen (nitrate and ammonium) reaches concentrations of ≈ 3000 µg/L in the mixolimnion, and between 1500 and 2000 µg/L in the monimolimnion (Fig. 7a, b). The concentration of phosphate phosphorus is ≈ 700 µg/L in the mixolimnion and reaches peak values of 2100 µg/L at a depth of 17 m (Fig. 7c). These values are much higher than those commonly reported for Lusatian coal mine pit lakes (0.8–6.5 µg/L N_t and 8–78 µg/L P_t; Nixdorf et al. 1998) and those reported in the mixolimnion of other metal mine pit

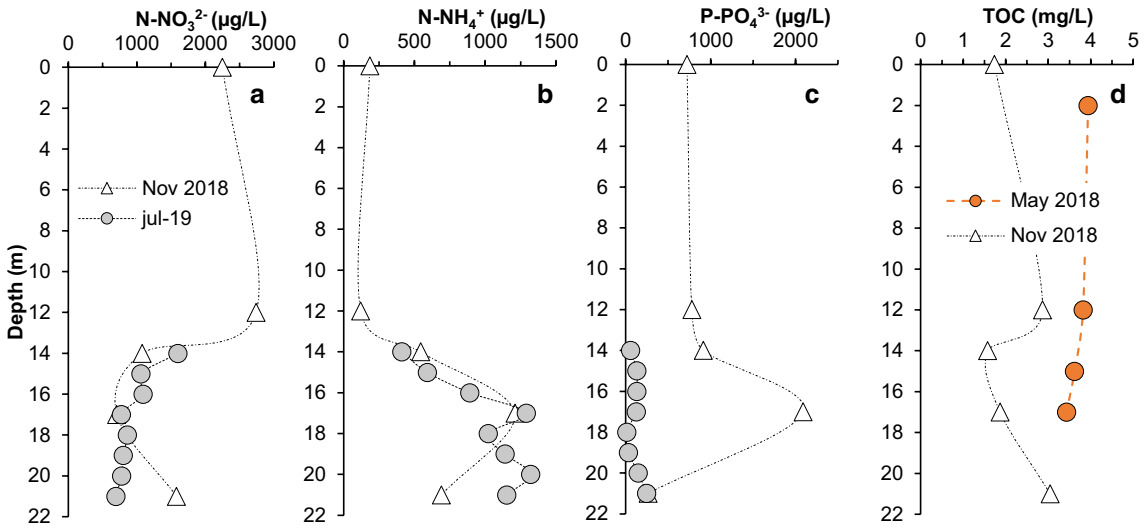

Fig. 7 Depth profiles of nitrate nitrogen (N-NO_3^{2-}), ammonium nitrogen (N-NH_4^+), phosphate phosphorus (P-PO_4^{3-}) and total organic carbon (TOC) obtained in Brunita acidic pit lake

lakes, such as those of the Iberian pyrite belt (600–800 µg/L N_t and < 50 µg/L P_t; Sánchez-España et al. 2013).

These concentrations are only comparable to those found in the deep part of the nutrient-rich and highly productive Cueva de la Mora pit lake (Wendt-Potthoff et al. 2012), in which an intense bacterial sulfate reduction layer was also reported (Diez-Ercilla et al. 2014). According to these nutrient concentrations, the Brunita pit lake is eutrophic (Wetzel 2001). Therefore, despite its high acidity and metal content, this pit lake has an important availability of basic nutrients to sustain a cascade of microbial interactions, as suggested in Sánchez-Andrea et al. (2011) for Rio Tinto sediments.

The high phosphate concentration has probably resulted from the dissolution of phosphate minerals present in the pit, such as vivianite and ludlamite (Cánovas et al. 2013), which are both readily soluble at low pH. The source of the nitrogen is currently unknown, but atmospheric deposition seems a plausible option, considering the high nitrate concentrations reported in local rainwater (4–23 mg/L NO_3^-; Alcolea et al. 2015). In any case, the inverse behavior of nitrate and ammonium in the pit lake (nitrate abundant in the mixolimnion and ammonium dominant in the monimolimnion) suggests a probable nitrogen cycle catalyzed by microorganisms. This is worth noting since both nitrification and dissimilatory nitrate reduction to ammonium (DNRA) are both considered to be precluded at very low pH. Jeschke et al. (2013) stated that the pH limit for nitrification is around 3.0, whereas the pH of the Brunita pit lake's mixolimnion is between 2.0 and 2.6. Regarding DNRA, Rütting et al. (2011) found an inconsistent relation of this bacterial metabolism with pH, since DNRA has been also observed at pH < 4 in poorly drained soils. In any case, nitrogen cycling has been also confirmed in enrichment cultures at low pH (Sánchez-Andrea et al. 2012) and even in sulfate-reducing bacteria isolated from the Rio Tinto (Sánchez-Andrea et al. 2015). The decrease in total organic carbon from May to November 2018 could indicate consumption by heterotrophic bacteria during the summer period (Fig. 7d).

Dissolved Gases and Water Density

Given the abundance of carbonates in the open pit (e.g. siderite, dolomite; Cánovas et al. 2013; López-García et al. 1992) and their continuous dissolution by acidic water, carbon dioxide could be generated and accumulated due to the meromictic character of this lake (little or no mixing or lake turnover). The solubility limit of CO_2 (aq.) is determined by absolute pressure and represents the level above which dissolved gases start forming bubbles. This process can destabilize lake stratification and trigger a limnic eruption (Halbwachs et al. 2004). Extremely high CO_2 concentrations have been detected in the Guadiana pit lake in Huelva (SW Spain), which is being degassed at this moment to reduce safety risks in the mining area (Boehrer et al. 2016; Sánchez-España et al. 2014b).

To evaluate the possible risk of carbon dioxide accumulation, the TDG profiles given in Fig. 3f were transformed to bar units and compared with the absolute pressure (Fig. 8a). Although the total pressure of dissolved gases certainly increases at depth (peak values of 1.5 bar below depths of 18 m; Fig. 8), this parameter is still far from the absolute pressure (atmospheric plus hydrostatic pressure) corresponding to that depth (2.8 bar). While the dominant dissolved gases in the mixolimnion are O_2 and N_2, the dissolved gases

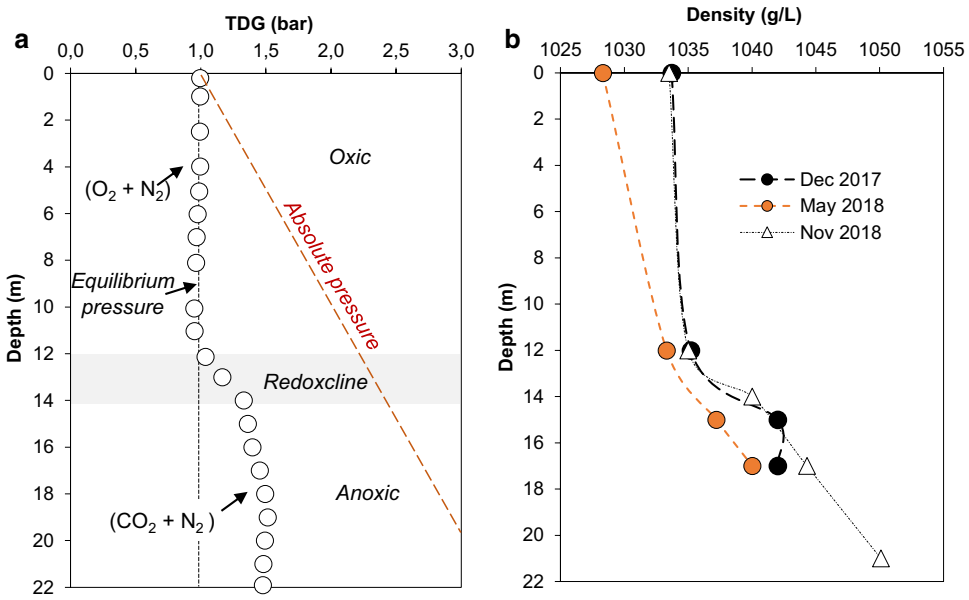

Fig. 8 **a** Vertical variation of total dissolved gas pressure (TDG, in bar) measured in November 2018; **b** density (in g/L) calculated for three different seasons (density calculations conducted with RHOMV, after Boehrer et al. 2010)

in the monimolimnion would be dominated by CO_2, with minor amounts of N_2 (perhaps plus trace contents of H_2S of biogenic origin). Precise concentrations of the different gases are not yet available. However, by comparison with the available data from the CO_2-charged acidic pit lake of Guadiana mine (Boehrer et al. 2016; Sánchez-España et al. 2014b), and assuming that CO_2 is by far the major dissolved gas at depth (so that total pressure could be almost entirely ascribed to the partial pressure of CO_2), we hypothesize that CO_2 concentrations in the deep part of the Brunita acidic pit lake could be in the range of 2000–2500 mg/L (45–57 mM CO_2).

In addition to the dissolved gases content, we have calculated the water density based on water temperature and solute concentrations (given in Figs. 4, 5, 6) and applied the RHOMV model for lake density calculations from Boehrer et al. (2010). As shown in Fig. 8b, the density profiles show a stable stratification of the water column with an important density increase below the redoxcline/chemocline (from 1030 to 1035 g/L at 12 m to around 1040–1045 g/L at 14–16 m, and up to 1050 g/L at 21 m). This vertical gradient of increasing density appears sufficient to avoid winter turnover. Even if the mixolimnion cools down to temperatures of around 10 °C, its hypothetical density (ca. 1036 g/L) would never equal that of the monimolimnion, and therefore, mixing would not affect the bottommost layer. This is consistent with the aforementioned accumulation of reduced substances (e.g. Fe(II) and dissolved gases (CO_2) in the pit lake bottom.

These density measurements do not account for the dissolved gas phase, as it has not been precisely quantified. The contribution of dissolved gases to density, however, is usually low (Boehrer et al. 2016) and would not change substantially with respect to values given in Fig. 8. In the particular case of CO_2, this gas contributes positively to density and thus helps to increase stratification stability (Boehrer et al. 2016). For example, a hypothetical concentration of 2000 mg/L CO_2 in the deepest water layer at 21 m would only increase the calculated density from around 1050 g/L to 1050.4 g/L.

Composition of Suspended Particulate Matter and Bottom Sediments

Electron microscopy investigation of SPM retained on filters revealed important differences in the mineralogical nature of suspended mineral particles in the Brunita acidic pit lake. In the upper part of the water column, i.e. the oxygen-rich mixolimnion, we could only observe detrital particles (e.g. quartz, clay minerals, pyrite, barite; *not shown*) transported from the adjacent shores by the wind or runoff. Secondary minerals formed on site, including iron oxides and oxyhydroxidesulfates such as jarosite (containing K, Na, and H_3O^+), schwertmannite, or goethite, were also observed in the mixolimnion, as a result of Fe(III) precipitation in the upper water column.

When passing from the mixolimnion to the monimolimnion, the water color and transparency changed drastically from deep red and slightly turbid to highly transparent with light greenish color (Fig. 2e–f), indicating a clear redox transition. Despite the transparency of the water, however, the membranes used to filter water below depths of 14 m, and very especially from 17 m, appeared densely coated with a brownish hue. A turbidity profile obtained in July 2019 (Fig. 9) showed the absence of measurable turbidity in the mixolimnion (upper 14 m of the water column) and

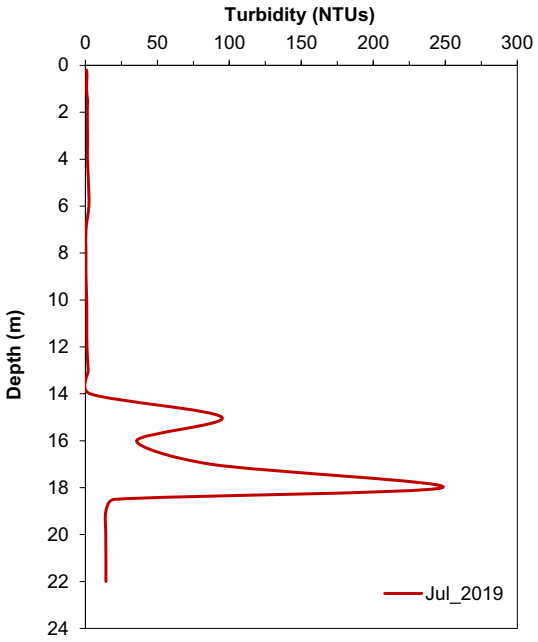

Fig. 9 Vertical evolution of turbidity (expressed in NTUs) measured along the water column of the Brunita acidic pit lake in July 2019

an intense turbidity maximum in the monimnolimnion, specifically in the layer between 14 and 18 m. This indicates the presence of very fine-grained, colloidal particles below the redoxcline that are almost imperceptible to the naked eye. Within this turbidity layer, which obviously delimits a horizon of high biogeochemical activity, two different sub-peaks can be distinguished (Fig. 9): a first maximum of 95 NTUs at 14 m, and a second, much higher maximum of 250 NTUs at 18 m. As described below, electron microscopy studies have revealed that these two sub-peaks correspond to an upper "iron turbidity" (minor peak) and a lower "sulfide turbidity" (major peak).

SEM investigations of the mineral coatings on the filters indicated that the colloidal particles at 14 m mostly consisted of *pin-cushion*-like schwertmannite (*not shown*), clearly suggesting Fe cycling in the oxic/anoxic transitional zone where the DO comes in contact with dissolved ferrous iron. On the other hand, most of the SPM found below 18 m consisted of spherical particles of zinc sulfide (ZnS), which were either dispersed or coalesced in groups of several spheres (Fig. 10a–d). The diameter of these sulfide particles was usually around 1 µm (Fig. 10a, b), though smaller ones in the range of 300–600 nm and even less were also observed (Figs. 10c–f, 11a, b). The chemical nature of these sulfides was revealed by EDS, which provided compositions almost exclusively consisting of Zn and S, sometimes incorporating Cd (Fig. 11b). TEM allowed us to observe some of these particles at a higher resolution and provided some clues about their possible crystalline nature (Fig. 11a). Electron diffraction (SAED) conducted on selected areas of these particles reveal a diverse degree of crystallinity, from diffuse rings typical of ultrafine or amorphous matter to rings with a limited number of spots, indicating the presence of crystalline nano-domains. Spacing measurements and their comparison with the American Mineralogist database (Downs and Hall-Wallace 2003) suggest that the zinc-sulfides are very likely wurtzite. Similar biogenic minerals related to sulfate-reducing bacteria have been previously observed by Druschel et al. (2002) and Moreau et al. (2004), among others. A possible explanation for these crystallographic features is that Zn first precipitates as amorphous ZnS (which would be thermodynamically favoured with respect to more crystalline forms) and that these particles gradually transform to more crystalline phases over time.

In addition to the sulfide particles, organic structures of unclear origin, but likely consisting of collapsed microbial cells, were commonly observed on the filters (Fig. 10e, f). These particles were found at 17 m, where ORP was at a minimum (e.g. -200 mV in December 2017; Fig. 3), pH values were maximum (e.g. 5.0 in May 2018; Fig. 3), and where TDG was at peak values (Fig. 8a). We contend that these geochemical features are indicative of intense microbiological activity dominated by sulfate-reducing bacteria, as discussed below.

A sample of bottom sediments (upper 2 cm) taken from the deepest point of the pit lake in May 2018 (Table 2) confirmed the above-referred mineralogical findings, providing a composition dominated by Al_2O_3, SiO_2, and Fe_2O_3 which is suggestive of the widespread presence of detrital aluminosilicates and chemical iron precipitates. This statement was confirmed by XRD analyses, which detected quartz, feldspar, clay minerals like illite and kaolinite, and also goethite (the latter probably resulting from aging of schwertmannite during early diagenesis; Regenspurg et al. 2004). In addition, the chemical analyses of these sediments yielded an abnormally high concentration of zinc (61,125 ppm Zn, equivalent to 6.1 wt%) and lead (3080 ppm Pb). Due to the abundance of highly crystalline phases, we could not detect any poorly crystalline secondary sulfide; we assume that the accumulation of these metals in the sediments has resulted from a continuous "rain" of ZnS and PbS particles from the sulfidic layer present a few meters above the sediments.

Water/Mineral Equilibrium Calculations

The measured sulfate concentrations and ORP in the deep part of the lake did not predict measurable amounts of S^{2-} in the system. However, a typical "rotten-egg" smell and the finding of abundant sulfides in the lower turbidity layer strongly suggested the presence of biogenic H_2S in the system. Thus, an arbitrary concentration of 1 mg/L H_2S was assumed to calculate a saturation index (SI) value for the

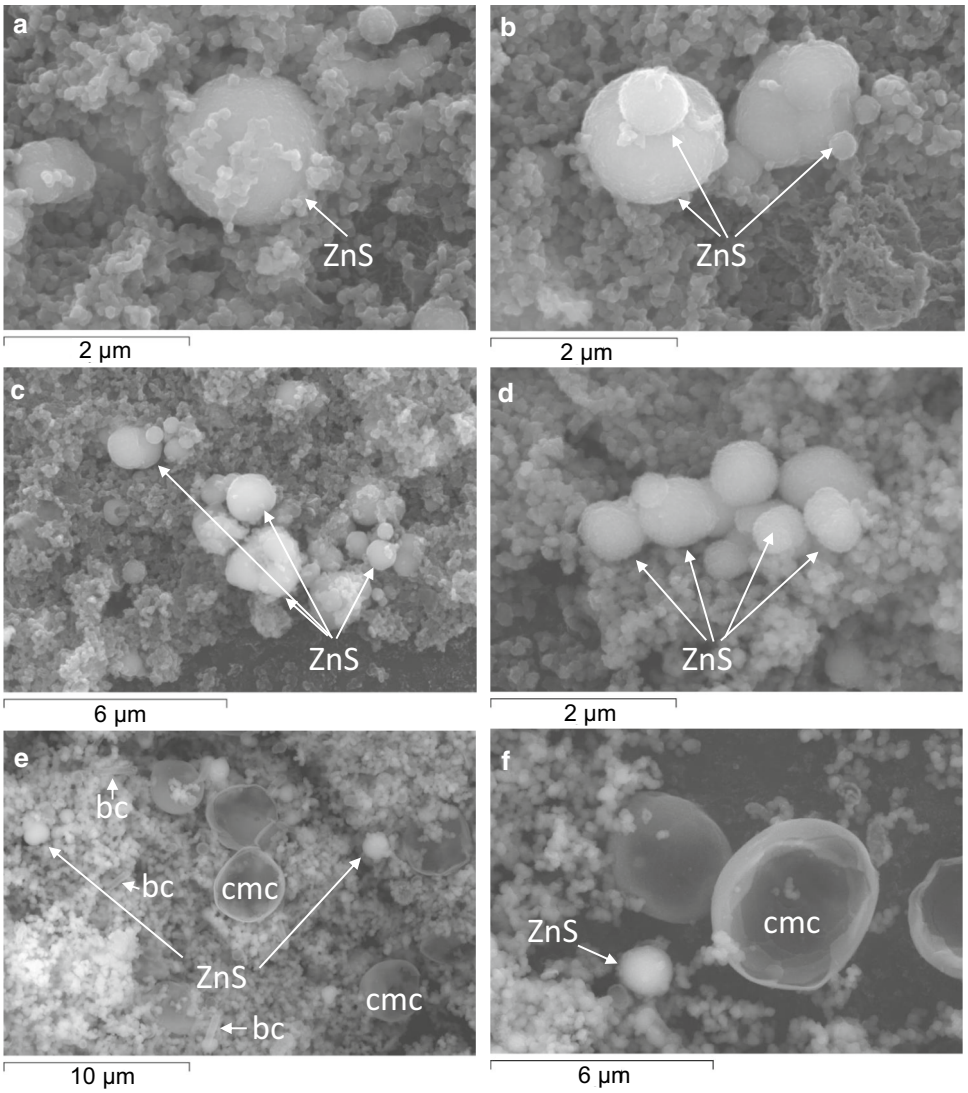

Fig. 10 SEM images of spherical particles of zinc sulfide (ZnS) found at depths of 15–17 m in the anoxic part of Brunita pit lake (**a–d**) and detail of sub-rounded organic structures resembling collapsed microbial cells (cmc) and bacillus-like bacteria (bc) coexisting with sparse ZnS particles (**e**, **f**)

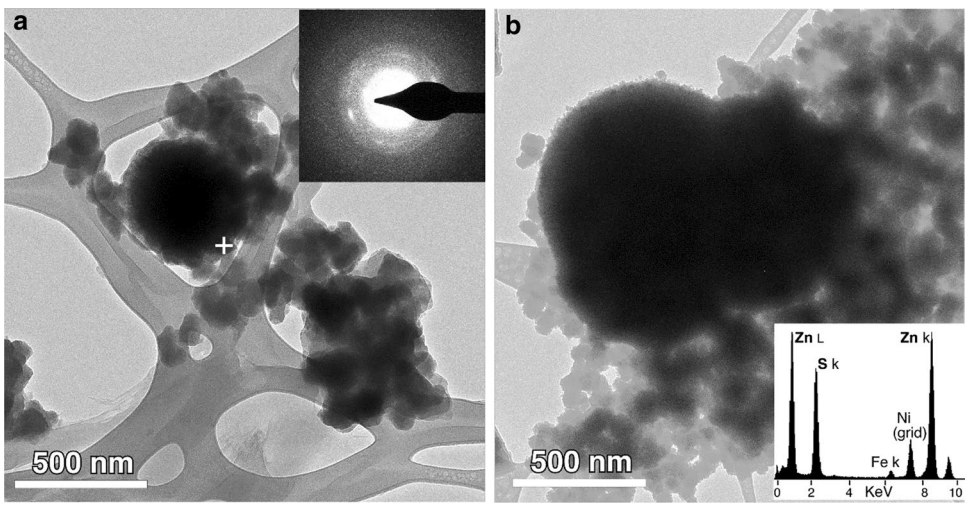

Fig. 11 TEM images of zinc sulfide particles found at 17 m depth in the acidic pit lake of Brunita mine. The selected area electron diffraction (SAED) pattern (corresponding to the point marked with a cross symbol) is shown in (**a**), whereas an EDS spectrum of coalescing particles is shown in (**b**)

Table 2 Chemical composition (XRF, ICP-MS) of bottom sediment (upper 2 cm) from Brunita pit lake

Major oxides		Trace elements	
	(%wt.)		(ppm)
SiO_2	19.2	As	124
Al_2O_3	12.8	Cd	227
Fe_2O_3	21.2	Co	9
CaO	0.92	Cr	46
TiO_2	0.38	Cu	32
MnO	0.38	Ni	20
K_2O	1.78	Pb	3080
MgO	2.71	Sb	20
P_2O_5	0.12	V	80
Na_2O	0.46	Y	47
LOI	30.47	Zn	61,125

Table 3 Saturation indices (SI) of selected mineral phases (aluminum oxy-hydroxides, metal sulfides, and other phases) as calculated for the deep, anoxic waters (17 m) of Brunita pit lake

Mineral phase	Formula	SI
Metal sulfides		
Covellite	CuS	7.88
Galena	PbS	1.71
Greenockite	CdS	2.32
Wurtzite	ZnS	2.04
Sphalerite	ZnS	4.54
ZnS (am.)	ZnS	2.14
$NiS_{(gamma)}$	NiS	4.39
$NiS_{(beta)}$	NiS	2.69
$CoS_{(beta)}$	CoS	1.94
Orpiment	As_2S_3	−3.55
Mackinawite	FeS	−1.76
$FeS_{(ppt)}$	FeS	−2.41
Aluminum oxy-hydroxides		
Basaluminite	$Al_4SO_4(OH)_{10}{\cdot}5H_2O$	−2.80
Jurbanite	$Al(SO_4)OH{\cdot}5H_2O$	0.41
Gibbsite	$Al(OH)_3$	−0.70
Diaspore	AlOOH	0.70
$Al(OH)_3$ am.	$Al(OH)_3$	−3.23
Others		
Gypsum	$CaSO_4{\cdot}2H_2O$	0.27
Mirabilite	$Na_2SO_4{\cdot}10H_2O$	−3.95
Native sulfur	S	15.56
Halite	NaCl	−5.08

The calculations assumes an arbitrary concentration of 1 mg/L H_2S in the system

sulfide minerals. The results of the PHREEQC calculations (Table 3) suggest that, with the exception of iron sulfides (e.g. pyrite, mackinawite, FeS_{ppt}) and arsenic sulfides (e.g. As_2S_3), which are apparently undersaturated, the deep waters of Brunita pit lake seem to be strongly oversaturated with respect to most other metal sulfides, including CuS, PbS, ZnS, NiS, and CoS. In practical terms, and considering that the presence of S^{2-} was set arbitrarily and not actually measured, these results imply that, at the observed geochemical conditions in the deep part of the lake, any small amount of H_2S produced by the sulfate-reducing bacteria would invariably react with the dissolved metals, leading to the formation of metal sulfides.

The fact that we could only find ZnS particles in the sulfidic layer despite having geochemical conditions favoring the precipitation of many other metal sulfides may be due to the extremely high concentrations of dissolved Zn in these waters (400–440 mg/L) relative to most other metals (e.g. 0–25 mg/L Cu, and ≈ 25 µg/L Pb, 50 µg/L, 600 µg/L Co, or 800 µg/L Ni). Even if these metal sulfides could have actually formed, they would be extremely difficult to find by EDS-SEM in the SPM due to their relative scarcity and small particle size. In the case of metals like Cu, Cd, or Pb, their low to undetectable concentrations probably resulted from their continuous precipitation as sulfide minerals over a long period of time.

The geochemical calculations also indicate near-equilibrium with respect to certain aluminum phases such as gibbsite or diaspore (Table 3), suggesting that the concentration of Al in this layer may be buffered and controlled by the solubility of some of these phases. In contrast, some other minerals commonly found in AMD environments, such as basaluminite or amorphous Al hydroxide, show very negative values (Table 3) and do not appear to play a relevant role in the control of Al solubility.

Other interesting features shown by the PHREEQC calculations are the apparent equilibrium to slight saturation with respect to gypsum solubility (SI = 0.27), which is in good agreement with the aforementioned widespread presence of gypsum crystals in the pit lake; the oversaturation with respect to elemental sulfur (SI = 15.56); or the evident undersaturation with respect to sodium- and chloride-containing minerals such as halite (SI = −5.08) or mirabilite (SI = -3.95) (Table 3). The undersaturation with respect to the latter minerals is worth noting, since the decrease in both sodium and chloride concentrations with depth (Fig. 5e, f) without an apparent remobilization mechanism such as mineral precipitation suggest that the vertical geochemical profiles for these two elements could be just pointing to a continuous input of salts to the pit lake surface in the form of atmospheric deposition (Alcolea et al. 2015).

Microbial Community Analysis

The microbial community was analyzed at depths of 2, 12, and 17 m, representative of the mixolimnion, chemocline, and monimolimnion, respectively (Table 4). The community

Table 4 Microbial community composition determined through 16S rRNA gene amplicon sequencing in the water column at 2, 12, and 17 m depth in Brunita Pit Lake

Bacterial taxonomy (Phylum_Class_Order_Family_Genus)	2 m	12 m	17 m
Proteobacteria_Alphaproteobacteria_Acetobacterales_Acetobacteraceae_Acidiphilium	0.511	0.034	0.008
Proteobacteria_Gammaproteobacteria_Gammaproteobacteria Incertae Sedis_Unknown Family_Acidibacter	0.154	0.046	0.003
Acidobacteria_Acidobacteriia_Acidobacteriales_Acidobacteriaceae (Subgroup 1)	0.074	0.005	-
Proteobacteria_Alphaproteobacteria_Acetobacterales_Acetobacteraceae	0.063	0.045	0.001
Nitrospirae_Nitrospira_Nitrospirales_Nitrospiraceae_Leptospirillum	0.06	0.045	0.002
Proteobacteria_Gammaproteobacteria_Betaproteobacteriales_Nitrosomonadaceae	0.046	0.032	0.034
Acidobacteria_Acidobacteriia_Acidobacteriales_Acidobacteriaceae (Subgroup 1)_Occallatibacter	0.040	0.006	-
Actinobacteria_Acidimicrobiia_Acidimicrobiales_Acidimicrobiaceae_Ferrithrix	0.025	0.002	-
Proteobacteria_Gammaproteobacteria_Xanthomonadales_Rhodanobacteraceae_Metallibacterium	0.012	0.033	-
Proteobacteria_Gammaproteobacteria_Acidithiobacillales_Acidithiobacillaceae_Acidithiobacillus	0.006	0.091	0.029
(Archaea) Euryarchaeota_Thermoplasmata_Thermoplasmatales_Thermoplasmataceae	-	0.302	-
Firmicutes_Bacilli_Bacillales_Alicyclobacillaceae_Acidibacillus	-	0.143	0.003
Proteobacteria_Alphaproteobacteria_uncultured	-	0.075	0.002
Proteobacteria_Gammaproteobacteria_Betaproteobacteriales_Burkholderiaceae_Thiomonas	-	0.071	0.005
Proteobacteria_Deltaproteobacteria_Syntrophobacterales_Syntrophaceae_Desulfobacca	-	0.006	0.046
Bacteroidetes_Bacteroidia	-	-	0.316
Bacteroidetes_Ignavibacteria_Ignavibacteriales	-	-	0.125
Proteobacteria_Deltaproteobacteria_Syntrophobacterales_Syntrophaceae_Desulfomonile	-	-	0.123
Bacteroidetes_Bacteroidia_Bacteroidales_Prolixibacteraceae_WCHB1-32	-	-	0.063
Patescibacteria_ABY1_Candidatus Falkowbacteria	-	-	0.046
Firmicutes_Clostridia_Clostridiales_Peptococcaceae_Desulfurispora	-	-	0.035
Bacteroidetes	-	-	0.026
Bacteroidetes_Bacteroidia_Bacteroidales_Paludibacteraceae	-	-	0.023
Actinobacteria_Thermoleophilia_Gaiellales_uncultured	-	-	0.022
Firmicutes_Negativicutes_Selenomonadales_Veillonellaceae_uncultured	-	-	0.006
Firmicutes_Clostridia_Clostridiales_Peptococcaceae_Desulfosporosinus	-	-	0.005
Proteobacteria_Gammaproteobacteria_Betaproteobacteriales_Hydrogenophilaceae_Thiobacillus	-	-	0.003
Proteobacteria_Deltaproteobacteria_Desulfobacterales_Desulfobulbaceae	-	-	0.002

Bold: genera harboring known sulfate reducing species. OTU abundance was quantified numerically, after removal of chloroplast and mitochondrial sequences; the intensity of green color correlates with abundance; blank spaces marked with (−) denote non-detection

diversity increased with depth; 10, 15, and 23 OTUs were detected in the mixolimnion, chemocline, and monimolimnion, respectively (Table 4). The increased diversity in the monimolimnion matched the observed attenuation of several physicochemical characteristics in this layer: an increase in pH, decreased sodium and chloride concentrations, and a drastic decrease in the concentrations of some metals (e.g. Cu, Cd, Cr, Pb, Th; Fig. 6).

In the oxic mixolimnion (2 m), more than half of the reads (51.1%) were assigned to the genus *Acidiphilium*, and 15.4% to the genus *Acidibacter*. Both genera harbour heterothrophic aerobic respirers that are also capable of catalysing Fe(III) reduction in microaerophilic and anaerobic conditions (Falagán et al. 2014). Their major presence in the oxic layer likely indicates their heterotrophic and aerobic respiratory metabolism, rather than iron reduction. Other heterotrophs were also present at significant amounts in the oxic layer (*Acidobacteraceae* members*, Acetobacteraceae, Occallatibacter,* or *Metallibacterium*). Heterotrophic microorganisms are thought to have a detoxifying role in low pH environments since they consume organic matter that is reported to inhibit certain chemolithoautotrophic microorganisms like acidophilic iron oxidizers (Johnson 1998). It is worth mentioning that typically the microbial composition of an AMD water column is dominated by iron oxidizers (e.g. González-Toril et al. 2015). In this pit lake, genera known to harbor iron oxidizers were detected, but their abundance in the upper layer was relatively low: *Leptospirilum*

(6%), *Acidithiobacillus* (0.6%), and *Ferrithrix* (2.5%). The low abundance of *Acidithiobacillus*-related sequences is surprising since they usually dominate AMD waters. Apart from the eutrophic conditions in the lake, a possible explanation could be that the physicochemical characteristics in this pit lake are more extreme than other AMD environments (Table 1). The combination of a very low pH (close to 2.0 in certain seasons; Fig. 3c) with a very high concentration of potentially toxic metals (e.g. Cu or Zn; Fig. 4c, d), and salinization by sodium chloride (Fig. 4e, f) could simultaneously be introducing multiple environmental stressors with drastic consequences for some of these microorganisms. For example, Bond et al. (2000a, b) argued that *Acidithiobacillus* sp. are outcompeted by *Leptospirilum* spp. at lower pH and higher concentrations of such metals.

In the redoxcline (12 m), heterotrophic growth and iron reduction seem to dominate. Microorganisms from the archaeal family *Thermoplasmataceae* were the most abundant OTU in this layer (30.2%), while they were absent in the top and bottom layers. *Thermoplasma* spp. are one of the very few *Archaea* commonly found in AMD environments (Baker and Banfield 2003). They are typically known for their facultative anaerobic heterotrophic metabolism, suggesting a potential fermentative pathway in this layer, although the low 16S rRNA gene identity with closest isolates make any presumption of their metabolism merely speculative. As is typical for AMD environments, iron metabolism, specifically Fe(III) reduction, plays an important role in this layer where oxygen has been consumed: the second and third most abundant OTUs belong to *Acidibacillus* (14.3%) and *Acidithiobacillus* (9.1%), genera known for iron metabolism in AMD environments (Baker and Banfield 2003; González-Toril et al. 2015). Overall, 39.5% of the OTUs in this layer were potential iron reducers (*Acidibacter, Acidiphilium, Ferrithrix*).

In the lower and reducing layer, heterotrophic, fermentative growth also likely plays an important role: 56.4% of total reads were assigned to OTU's in the phylum *Bacteroidetes*. This phylum harbours many heterotrophs capable of fermentation, which could explain their dominance in this anaerobic environment in the presence of organic carbon settling from the upper layer. As an example, *Microbacter margulisiae*, which belongs to the OTUs identified as *Paludibacteraceae* within *Bacteroidetes*, was isolated from the Rio Tinto, showing mainly fermentative growth (Sánchez-Andrea et al. 2014). Overall, the high abundance of heterotrophic microorganisms in the water column, compared to other AMD waters, could point to the influence of the limited water–mineral contact area, which provides less surface area for chemolithoautotrophic microorganisms to thrive. It should also be noted that eukaryotic sequences, classified by mitochondrial and chloroplast DNA, dominated the upper and middle layers—45.1% and 48.4% of filtered reads, respectively—but were not detected in the bottom layer. These sequences were not taken into account for determination of relative microbial OTU abundance due to their eukaryotic origin. However, the presence of chloroplasts points to the important role of photosynthetic microorganisms like algae as primary producers in the upper layer, providing a source of organic carbon along the water column as dead cells settle. Sequences related to the genera *Thiomonas*, which are typically found in AMD environments, made up to 7.1% of the total reads in this 12 m sample. *Thiomonas* spp. 3A possesses the genes for nitrate reduction (Arsène-Ploetze et al. 2010) and *Thiomonas arsenivorans* is able to oxidize As(III) (Battaglia-Brunet et al. 2006). Although their role cannot be demonstrated at this moment, their higher abundance in this oxygen-depleted layer suggests the participation of *Thiomonas* in anaerobic respiration at depth.

While absent from the top layer and present in very low numbers in the redoxcline (0.6%), sulfate-reducing bacteria (SRB) were abundant at 17 m depth, making up 21.2% of the OTU's: *Desulfomonile* (12.3%), *Desulfobacca* (4.6%), *Desulfurispora* (3.5%), *Desulfosporosinus* (0.5%), and *Desulfobulbaceae* (0.2%). This high relative abundance of SRB at 17 m, together with the complete removal of Cu^{2+}, partial removal of Zn^{2+}, and the observation of ZnS particles in the water column at this depth, strongly point towards sulfidogenic activity as the main factor causing metal attenuation at the bottom of this pit lake. In addition, anaerobic reductive respiratory processes in general, and sulfate reduction in particular, have been shown to increase the pH in low-pH culture conditions (Sánchez-Andrea et al. 2015); this is reflected in the pH increase in the bottom layer, which also facilitates metal precipitation.

Geomicrobiological and Biotechnological Implications

For a long time, there was a general consensus that microbial sulfate reduction was inhibited in acidic environments with pH < 5 (Hao et al. 1996; Widdel 1988). The most accepted idea was that these microorganisms have a low metabolic energy yield (Hamilton 1998), which makes them especially susceptible to low pH. In addition, metabolic products of these anaerobic bacteria, such as H_2S and organic acids, are known to be potentially toxic at a low pH. However, it is now well established that SRB can exist at a much lower pH, as long as sufficient carbon exists in the system (Koschorreck 2008). SRB have been reported in different low pH-environments, such as peatlands (Pester et al. 2010), macroscopic microbial streamers and mats (Rowe et al. 2007), freshwater sediments impacted with AMD (Herlihy and Mills 1985), acidic pit lake sediments (Koschorreck et al. 2003; Rüffel et al. 2018), acidic mine tailings in Canada (Praharaj and Fortin 2004), Chile (Diaby et al. 2007), and Siberia

(Karnachuk et al. 2005), moderately acidic (pH ≈ 4) sediments around flooded mine workings in the USA (Church et al. 2007), and Rio Tinto sediments in Spain (Sánchez-Andrea et al. 2011, 2013). However, although this is still a matter of some controversy, in all of these reports, sulfate reducers could possibly perform sulfidogenesis in less acidic micro-niches, and therefore did not necessarily need to be tolerant of extreme acidity. As a matter of fact, so-far described acidophilic SRB are moderate acidophiles growing poorly below pH 4 (Sánchez-Andrea et al. 2015). Two other reports suggested SRB in the water column of an acidic pit lake (Diez-Ercilla et al. 2014; Falagán et al. 2015) and SRB sequences were found in mine water with high uranium concentrations (Giloteaux et al. 2013).

The SRB detected in the Brunita pit lake are present in the water column, unprotected from the extreme conditions, and dealing with high dissolved metal concentrations, high salinity, and high ionic strength. To our knowledge, this is the first report where sequences of several SRB genera were detected in a stratified water column with a tight link to a change in the physico-chemical characteristics and self-mitigation of the extreme conditions. Moreover, so far there is no described acidophilic SRB in the *Proteobacteria* class; hence, the high abundance of *Desulfomonile* and *Desulfobaca*-related sequences indicates that this pit lake may be an excellent resource for isolation of highly resistant and novel acidophilic SRB. Such SRB could be highly valuable for metal recovery and bioremediation of AMD (Sánchez-Andrea et al. 2014). SRB have been shown to be very efficient in bioreactors treating acid mine drainage (Nancucheo et al. 2017). These microorganisms have been shown to be effective scavengers of dissolved toxic elements such as aluminum or arsenic, either with isolated strains (Rüffel et al. 2018) or using a consortium of different species (Falagán et al. 2017b; Le Pape et al. 2017). Moreover, SRB can be used to selectively precipitate valuable metals like Cu or Zn from AMD (Nancucheo et al. 2012). Thus, the search for novel SRB that can operate at more severe chemical conditions is currently of clear biotechnological interest.

Conclusions

We have shown that the combination of detailed physico-chemical profiles with microbiological research is a powerful tool to reveal the key microbial players in element (C, S, Fe, N) cycling in highly acidic and metal-rich pit lakes. The DO concentrations, TOC measurements, and 16S rRNA gene amplicon sequencing, along with visual observations, reinforce the idea of an important photosynthetic contribution for primary production by algae in the ecosystem. The measured concentrations of basic nutrients (nitrogen, phosphorus) place this pit lake as eutrophic, in contrast with most AMD systems or pit lakes, which are usually oligotrophic (Wendt-Potthoff 2013). Decaying phytoplanktonic biomass seems to be a good carbon source for heterotrophic bacteria, as reflected in the abundance of heterotrophic microorganisms in the water column performing different anaerobic respiratory processes. We observed perfect zonation, from oxygen reducers, to iron reducers, and sulfate reducers in the Brunita pit lake water column. As anaerobic reduction takes place, the pH increases to about 4.5–5.0, which allows a higher diversity of microorganisms. In addition, the sulfate reduction chemically alleviates the metal toxicity by metal sulfide precipitation, as confirmed by geochemical profiles and SEM observations. This represents an outstanding example of how the microbial metabolism of SRB can detoxify and self-mitigate a heavily polluted water body, despite its apparently extreme chemical conditions.

Acknowledgements This study was funded by the Spanish Ministry of Economy, Industry and Competitiveness through the National Research Agency (FEDER funds, Grant CGL2016-74984-R). We thank our colleagues from the IGME laboratories (Jesús Reyes, Ana Nieto, Mercedes Castillo, Maite Andrés) for chemical analyses of waters and sediments. We thank the personnel at the SGIker facilities of the Basque Country University (Javier Sanguesa, Ana Martínez-Amesti, and Sergio Fernández) for their help during mineralogical characterization. ISA was funded by the Netherlands Organisation for Scientific Research (NWO) through SIAM Gravitation grant 024.002.002. We thank Iame Alves Guedes for processing the filter samples, and two anonymous reviewers for their helpful suggestions on an earlier version of this manuscript.

References

Alcolea A, Fernández-López C, Vázquez M, Caparrós A, Ibarra I, García C, Zarroca M, Rodríguez R (2015) An assessment of the influence of sulfidic mine wastes on rainwater quality in a semi-arid climate (SE Spain). Atmos Environ 107:85–94

Arsène-Ploetze F, Koechler S, Marchal M, Coppée JY, Chandler M, Bonnefoy V, Bruneel O (2010) Structure, function, and evolution of the *Thiomonas* spp. genome. PLoS Genet 6(2):e1000859

Baker BJ, Banfield JF (2003) Microbial communities in acid mine drainage. FEMS Microbiol Ecol 44(2):139–152

Ball JW, Nordstrom DK (1991) User's manual for WATEQ4F, with revised thermodynamic data base and test cases for calculating speciation of major, trace, and redox elements in natural waters. USGS Open-file Report 91-183, Washington DC

Battaglia-Brunet F, Joulian C, Garrido F, Dictor MC, Morin D, Coupland K, Baranger P (2006) Oxidation of arsenite by *Thiomonas* strains and characterization of *Thiomonas arsenivorans* sp. nov. Antonie Van Leeuwenhoek 89(1):99–108

Boehrer B, Herzsprung P, Schultze M, Millero FJ (2010) Calculating density of water in geochemical lake stratification models. Limnol Oceanogr-Meth 8:567–574

Boehrer B, Magin K, Yusta I, Sánchez-España J (2016) Quantifying, assessing and removing extreme gas load from meromictic Guadiana pit lake, Southwest Spain. Sci Total Environ 563–564:468–477

Bond PL, Smriga SP, Banfield JF (2000a) Phylogeny of microorganisms populating a thick, subaerial, predominantly lithotrophic

biofilm at an extreme acid mine drainage site. Appl Environ Microbiol 66(9):3842–3849
Bond PL, Druschel GK, Banfield JF (2000b) Comparison of acid mine drainage microbial communities in physically and geochemically distinct ecosystems. Appl Environ Microbiol 66:4962–4971
Cánovas M, Alhama I, López G (2013) La paragénesis mineralógica de la Cantera "Brunita". In: de Jornadas VI (ed), Introducción a la investigación de la UPCT, Investigación EICM, Nº 6, pp 40–42, ISSN 1888-8356 **(in Spanish)**
Church CD, Wilkin RT, Alpers CN, Rye RO, McCleskey RB (2007) Microbial sulfate reduction and metal attenuation in pH 4 acid mine water. Geochem Trans 8:10
Diaby N, Dold B, Pfeifer HR, Holliger C, Johnson DB, Hallberg KB (2007) Microbial communities in a porphyry copper tailings impoundment and their impact on the geochemical dynamics of the mine waste. Environ Microbiol 9:298–307
Diez-Ercilla M, López-Pamo E, Sánchez-España J (2009) Photoreduction of Fe(III) in the acidic mine pit lake of San Telmo (Iberian pyrite belt): field and experimental work. Aq Geochem 15(3):391–419
Diez-Ercilla M, Sánchez-España J, Yusta I, Wendt-Potthoff K, Koschorreck M (2014) Formation of biogenic sulfides in the water column of an acidic pit lake: biogeochemical controls and effects on trace metal dynamics. Biogeochem 121(3):519–536
Downs RT, Hall-Wallace M (2003) The American Mineralogist crystal structure database. Am Miner 88:247–250
Druschel GK, Labrenz M, Thomsen-Ebert T, Fowle DA, Banfield JF (2002) Geochemical modeling of ZnS in biofilms: an example of ore depositional processes. Econ Geol 97(6):1319–1329
Eary LE, Castendyk DN (2013) Hardrock metal mine pit lakes: Occurrence and geochemical characteristics. In: Geller W, Schultze M, Kleinmann B, Wolkersdorfer C (eds) Acidic pit lakes: the legacy of coal and metal surface mines. Springer, Berlin, pp 75–106
Falagán C, Johnson DB (2014) *Acidibacter ferrireducens* gen. nov., sp. nov.: an acidophilic ferric iron-reducing gammaproteobacterium. Extremophiles 18(6):1067–1073
Falagán C, Johnson DB (2015) *Acidithiobacillus ferriphilus* sp. nov.: a facultatively anaerobic iron- and sulfur-metabolising extreme acidophile. Int J Syst Evol Microbiol 66(1):206–211
Falagán C, Sánchez-España J, Johnson DB (2014) New insights into the biogeochemistry of extremely acidic environments revealed by a combined cultivation-based and culture-independent study of two stratified pit lakes. FEMS Microbiol Ecol 87(1):231–243
Falagán C, Sánchez-España FJ, Yusta I, Johnson DB (2015) Microbial communities in sediments in acidic, metal-rich mine lakes: results from a study in south-west Spain. Adv Mat Res 1130:7–10
Falagán C, Sánchez-España J, Yusta I, Johnson DB (2016) New insights into the microbiology of meromictic acidic pit lakes in the Iberian pyrite belt (Spain). In: Drebenstedt Carsten, Paul Michael (eds) Mining meets water—conflicts and solutions, Proc, IMWA 2016 Conf. Freiberg, Germany, pp 192–198
Falagán C, Foesel BU, Johnson DB (2017a) *Acidicapsa ferrireducens* sp. nov., Acidicapsa acidiphila sp. nov., and Granulicella acidiphila sp. nov.: novel acidobacteria isolated from metal-rich acidic waters. Extremophiles 21(3):459–469
Falagán C, Sánchez-España J, Yusta I, Johnson DB (2017b) Biologically-induced precipitation of aluminium in synthetic acid mine water. Miner Eng 106:79–85
Friese K, Herzprung P, Schultze M (2013) Pit lakes from coal and lignite mining. In: Geller W, Schultze M, Kleinmann R, Wolkersdorfer C (eds) Acidic pit lakes—the legacy of coal and metal surface mines. Springer, Heidelberg, pp 42–57
Gammons CH, Tucci NJ (2013) The Berkeley pit lake, Butte, Montana. In: Geller W, Schultze M, Kleinmann R, Wolkersdorfer C (eds) Acidic pit lakes—the legacy of coal and metal surface mines. Springer, Heidelberg, pp 362–376
García C (2004) Impacto y riesgo ambiental de los residuos minero-metalúrgicos de la Sierra de Cartagena-La Unión (Murcia-España). PhD thesis. Univ Politécnica de Cartagena
Geller W, Schultze M, Wisotzky F (2013a) Remediation and management of acidified pit lakes and outflowing waters. In: Geller W, Schultze M, Kleinmann R, Wolkersdorfer C (eds) Acidic pit lakes—the legacy of coal and metal surface mines. Springer, Heidelberg, pp 225–264
Geller W, Schultze M, Kleinmann R, Wolkersdorfer C (2013b) Acidic pit lakes: the legacy of coal and metal surface mines. Springer, Heidelberg, p 525
Giloteaux L, Duran R, Casiot C, Bruneel O, Elbaz-Poulichet F, Goni-Urriza M (2013) Three-year survey of sulfate-reducing bacteria community structure in Carnoules acid mine drainage (France), highly contaminated by arsenic. FEMS Microbiol Ecol 83:724–737
González-Toril E, Santofimia E, López E, García-Moyano A, Aguilera A, Amils R (2015) Comparative microbial ecology of the water column of an extreme acidic pit lake, Nuestra Señora del Carmen, and the Río Tinto basin (Iberian pyrite belt). Int Microbiol 17(4):225–233
Halbwachs M, Sabroux JC, Granjeon J, Kayser G, Tochon-Danguy JC, Felix A, Beard JC, Villevieille A, Vitter G, Richon B, Wuest A, Hell J (2004) Degassing the "killer lakes" Nyos and Monoun, Cameroon. EOS 85(30):281–288
Hamilton WA (1998) Sulfate-reducing bacteria. Physiology determines their environmental impact. Geomicrobiol J 15:19–28
Hao OJ, Chen JM, Huang L, Buglass RL (1996) Sulfate-reducing bacteria. Crit Rev Environ Sci Technol 26:155–187
Herlihy AT, Mills AL (1985) Sulfate reduction in freshwater sediments receiving acid mine drainage. Appl Environ Microbiol 49:179–186
Jeschke C, Falagán C, Knoeller K, Schultze M, Koschorreck M (2013) No nitrification in lakes below pH 3. Environ Sci Technol 47:24
Johnson DB (1998) Biological abatement of acid mine drainage: the role of acidofilic protozoa and other indigenous microflora. Acidic Mining Lakes, Springer, pp 285–301
Karnachuk OV, Frank YA, Pimenov NV, Yusupov SK, Ivanov MV, Kaksonen AH, Puhakka JA, Lindström EB, Tuovinen OH (2005) Sulfate reduction potential in sediments in the Norilsk mining area, northern Siberia. Geomicrobiol J 22:11–25
Koschorreck M (2008) Microbial sulfate reduction at low pH. FEMS Microbiol Ecol 64:329–342
Koschorreck M, Wendt-Potthoff K, Geller W (2003) Microbial sulfate reduction at low pH in sediments of an acidic lake in Argentina. Environ Sci Technol 37:1159–1162
Kumar RN, McCullough CD, Lund MA (2013) Pit lakes in Australia. In: Geller W, Schultze M, Kleinmann R, Wolkersdorfer C (eds) Acidic pit lakes—the legacy of coal and metal surface mines. Springer, Heidelberg, pp 342–362
Le Pape P, Battaglia-brunet F, Parmentier M, Joulian C, Gassaud C, Fernández-Rojo L, Guigner J-M, Ikogou M, Stetten L, Olivi L, Casiot C, Morin G (2017) Complete removal of arsenic and zinc from a heavily contaminated acid mine drainage via an indigenous SRB consortium. J Hazard Mater 321:764–772
López-García JA, Manteca JI, Prieto AC, Calvo B (1992) Primera aparición en España de cronstedtita, Caracterización estructural. Bol Soc Esp Mineral 15(1):21–25
López-García JA, Oyarzun R, Manteca JI (2010) El distrito minero de La Unión: Plomo, zinc, plata y estaño en la Sierra de Cartagena. In: Lillo J, López I, López JA, Oyarzun R (Eds), *Geoguías GEMM* (*Grupo Estudios en Minería y Medioambiente*), Serie Distritos Mineros 3 (brochure downloaded from https://eprints.ucm.es/26229/)
López-Pamo E, Sánchez-España J, Diez M, Santofimia E, Reyes J (2009) Cortas mineras inundadas de la Faja Pirítica: Inventario

e hidroquímica. Serie Medio Ambiente 13, Instituto Geológico y Minero de España, Madrid

Manteca JI, Ovejero G (1992) Los yacimientos Zn, Pb, Ag-Fe del distrito minero de La Unión-Cartagena, Bética Oriental (Zn, Pb, Ag-Fe ore deposits of La Unión-Cartagena mining district, eastern Betic Cordillera). In: Martínez-Frías J (ed) García-Guinea J. Recursos minerales de España, CSIC, pp 1085–1101

Moreau JW, Webb RI, Banfield JF (2004) Ultrastructure, aggregation-state, and crystal growth of biogenic nanocrystalline sphalerite and wurtzite. Am Miner 89:950–960

Nancucheo I, Hedrich S, Johnson DB (2012) New microbiological strategies that enable the selective recovery and recycling of metals from acid mine drainage and mine process waters. Miner Mag 76(7):2683–2692

Nancucheo I, Bitencourt JAP, Sahoo PK, Alves JO, Siqueira JO, Oliveira G (2017) Recent developments for remediating acidic mine waters using sulfidogenic bacteria. Biomed Res Int 3:1–17

Nixdorf B, Mischke U, Lebmann D (1998) Chrysophites and chlamydomonas: pioneer colonists in extremely acidic mining lakes (pH < 3) in Lusatia (Germany). Hydrobiol 369(370):315–327

Nordstrom DK (2004) Modeling low-temperature geochemical processes. In: Holland HD, Turekian KK (eds) Treatise on Geochemistry, 2nd edit, vol 5. Surface and Ground Water, Weathering, and Soils. Elsevier Pergamon, Amsterdam, pp 37–72

Oen IS, Fernández JC, Manteca JI (1975) The lead-zinc and associated ores of La Unión, Sierra de Cartagena, Spain. Econ Geol 70:1259–1278

Parkhurst DL, Appelo CAJ (2013) Description of input and examples for PHREEQC version 3—a computer program for speciation, batch-reactions, one-dimensional transport, and inverse geochemical calculations. Groundwater Book 6, Modeling Techniques. USGS, Denver

Pavillon MJ (1969) Les minèralisations plombo-zinciferes de Carthagène (Cordilleres Betiques, Espagne). Miner Deposita 4:368–385

Pester M, Bittner N, Deevong P, Wagner M, Loy A (2010) A 'rare biosphere' microorganism contributes to sulfate reduction in a peatland. ISME J 4:1591–1602

Praharaj T, Fortin D (2004) Indicators o microbial sulfate reduction in acidic sulfide-rich mine tailings. Geomicrobiol J 21:457–467

Quast C, Pruesse E, Yilmaz P, Gerken J, Schweer T, Yarza P, Glöckner FO (2013) The SILVA ribosomal RNA gene database project: improved data processing and web-based tools. Nucleic Acids Res 41(D1):590–596

Ramiro-Garcia J, Hermes GDA, Giatsis C, Sipkema D, Zoetendal EG, Schaap PJ, Smidt H (2018) NG-Tax, a highly accurate and validated pipeline for analysis of 16S rRNA amplicons from complex biomes. F1000 Res 5:1791

Regenspurg S, Brand A, Peiffer S (2004) Formation and stability of schwertmannite in acidic mining lakes. Geochim Cosmochim Ata 68:1185–1197

Robles-Arenas VM, Rodríguez R, García C, Manteca JI, Candela L (2006) Sulfide-mining impacts in the physical environment: Sierra de Cartagena–La Unión (SE Spain) case study. Environ Geol 51:47–64

Rowe OF, Sánchez-España J, Hallberg KB, Johnson DB (2007) Microbial communities and geochemical dynamics in an extremely acidic, metal-rich stream at an abandoned sulfide mine (Huelva, Spain) underpinned by two functional primary production systems. Environ Microbiol 9:1761–1771

Rüffel V, Maar M, Dammbrück MN, Hauroeder B, Neu TR, Meier J (2018) *Thermodesulfobium* sp. strain 3baa, an acidophilic sulfate reducing bacterium forming biofilms triggered by mineral precipitation: Acidophilic sulfate reducer forming biofilms. Environ Microbiol 20(10):3717–3731

Rütting T, Boeckx Müller C, Klemedtsson L (2011) Assessment of the importance of dissimilatory nitrate reduction to ammonium for the terrestrial nitrogen cycle. Biogeosciences 8:1779–1791

Sánchez-Andrea I, Rodríguez N, Amils R, Sanz JL (2011) Microbial diversity in anaerobic sediments at Rio Tinto, a naturally acidic environment with a high heavy metal content. App Environ Microbiol 77:6085–6093

Sánchez-Andrea I, Rojas-Ojeda P, Amils R, Sanz JL (2012) Screening of anaerobic activities in sediments of an acidic environment: Tinto River. Extremophiles 16(6):829–839

Sánchez-Andrea I, Stams AJM, Amils R, Sanz JL (2013) Enrichment and isolation of acidophilic sulfate-reducing bacteria from Tinto River sediments. Environ Microbiol Rep 5(5):672–678

Sánchez-Andrea I, Sanz JL, Stams AJ (2014) *Microbacter margulisiae* gen. nov., sp. nov., a propionigenic bacterium isolated from sediments of an acid rock drainage pond. Int J Syst Evol Microbiol 64(12):3936–3942

Sánchez-Andrea I, Stams AJ, Hedrich S, Ňancucheo I, Johnson DB (2015) *Desulfosporosinus acididurans* sp. nov.: an acidophilic sulfate-reducing bacterium isolated from acidic sediments. Extremophiles 19(1):39–47

Sánchez-España J, Diez M (2008) Geochemical modeling of concentrated mine waters: a comparison of the Pitzer ion-interaction theory with the ion-association model for the study of melanterite solubility in San Telmo mine (Huelva, Spain). In: Stefansson O (ed) Geochemistry research advances. Nova Science, New York, pp 31–55

Sánchez-España J, López Pamo E, Santofimia E, Aduvire O, Reyes J, Barettino D (2005) Acid mine drainage in the Iberian pyrite belt (Odiel river watershed, Huelva, SW Spain): geochemistry, mineralogy and environmental implications. Appl Geochem 20–7:1320–1356

Sánchez-España J, López-Pamo E, Santofimia E, Diez-Ercilla M (2008) The acidic mine pit lakes of the Iberian Pyrite Belt: an approach to their physical limnology and hydrogeochemistry. Appl Geochem 23:1260–1287

Sánchez-España J, López-Pamo E, Diez M, Santofimia E (2009) Physico-chemical gradients and meromictic stratification in Cueva de la Mora and other acidic pit lakes of the Iberian pyrite belt. Mine Water Environ 28:15–19

Sánchez-España J, Yusta I, Diez-Ercilla M (2011) Schwertmannite and hydrobasaluminite: a re-evaluation of their solubility and control on the iron and aluminum concentration in acidic pit lakes. Appl Geochem 26:1752–1774

Sánchez-España J, Diez M, Santofimia E (2013) Mine pit lakes of the Iberian pyrite belt: some basic limnological, hydrogeochemical and microbiological considerations. In: Geller W, Schultze M, Kleinmann B, Wolkersdorfer C (eds) Acidic Pit Lakes: The Legacy of Coal and Metal Surface Mines. Springer, Heidelberg, pp 315–342

Sánchez-España J, Diez M, Cerdán FP, Yusta I, Boyce AJ (2014a) Hydrological investigation of a multi-stratified pit lake using radioactive and stable isotopes combined with hydrometric monitoring. J Hydrol 511:494–508

Sánchez-España J, Boehrer B, Yusta I (2014b) Extreme carbon dioxide concentrations in acidic pit lakes provoked by water/rock interaction. Environ Sci Technol 48:4273–4281

Schultze M, Boehrer B, Wendt-Potthoff K, Sánchez-España J, Castendyk D (2017) Meromictic pit lakes: case studies from Spain, Germany and Canada and general aspects of management and modelling. In: Gulati RD, Zadereev AE, Degermendzhi AG (eds) Ecology of Meromictic Lakes, Ecological Studies 228. Springer, New York, pp 235–275

Wendt-Potthoff K (2013) The biology and ecosystems of acidic pit lakes. In: Geller W, Schultze M, Kleinmann B, Wolkersdorfer C

(eds) Acidic Pit Lakes: the legacy of coal and metal surface mines. Springer, Heidelberg, pp 107–186

Wendt-Potthoff K, Koschorreck M, Diez M, Sánchez-España J (2012) High microbial activity in a nutrient-rich, acidic mine pit lake. Limnologica 42–3:175–188

Wetzel RG (2001) Limnology—lake and river ecosystems, 3rd edn. Elsevier, Amsterdam

Widdel F (1988) Microbiology and ecology of sulfate- and sulfur-reducing bacteria. In: Zehnder A (ed) Biology of Anaerobic Microorganisms. Wiley, New York City, pp 469–585

Yilmaz P, Parfrey LW, Yarza P, Gerken J, Pruesse E, Quast C, Glöckner FO (2014) The SILVA and "all-species Living Tree Project (LTP)" taxonomic frameworks. Nucl Acid Res 42(D1):643–648

Zurek R, Diakiv V, Szarek-Gwiazda E, Kosiba J, Wojtal AZ (2018) Unique pit lake created in an opencast potassium salt mine: (Dombrovska pit lake in Kalush, Ukraine). Mine Water Environ 37:456–469